International Journal of Concrete Structures and Materials

RESEARCH

Open Access

Progressive Collapse of Typical and Atypical Reinforced Concrete Framed Buildings

Solomon Abebe Derseh[1*], Tesfaye Alemu Mohammed[2,4] and Girum Urgessa[3]

Abstract

This paper investigates the progressive collapse potential of eight-story reinforced concrete framed buildings with several atypical structural configurations and compares results with a typical structural configuration. The alternative load path mechanism, the linear-static analysis procedure amplified by dynamic increase factors, and the demand capacity ratio criterion limits from the U.S. General Services Administration guideline were used to evaluate the vulnerability of the different atypical and typical framed structures. Variations in bay size, plan irregularity, and closely spaced columns were used to represent the atypical structural configurations. The extracted demand-capacity ratio (DCR) of the global structural response showed that the demand-capacity ratio for the longitudinal frame with short-span beams had a larger DCR than the transverse frame with longer beam spans with significant potential for progressive collapse. Furthermore, atypical building configurations with closely spaced columns failed by shear and showed the highest DCR limits. In addition to the global structural response, the local member end actions were also evaluated. The evaluation showed that the critical atypical frame configuration with closely spaced columns had a 91% and 127% maximum shear force and support bending moment value difference, respectively, when compared to a baseline typical frame configuration.

Article Highlights

- Longitudinal frame with short span beams has a higher progressive collapse risk than a transverse frame with longer beams.
- Atypical configurations with closely spaced columns shows shear failure mode and are most vulnerable to progressive collapse.
- The critical scenario for collapse is interior column loss due to a larger tributary loading area.

Keywords Atypical frame, Column removal, GSA guideline, Linear-static analysis, Progressive collapse, Typical frame

ISSN 1976-0485 / eISSN 2234-1315

*Correspondence:
Solomon Abebe Derseh
solomon_abebe@dmu.edu.et
Full list of author information is available at the end of the article

1 Introduction

Progressive collapse can be defined as a case where local failure of a primary structural component spreads to the collapse of adjoining structural members leading to additional partial or total collapse. The total damage is disproportionate to the original cause and requires both an abnormal loading to initiate the local damage and a structure that lacks adequate continuity, ductility, and redundancy to resist the spread of the damage (ASCE, 2007; DOC, 2007; DOD, 2009; Fu, 2016; GSA, 2003; Marchand & Alfawakhiri, 2004; Starossek, 2009).

Kiakojouri et al., (2020) described three requirements for disproportionate collapse succinctly. First, the initial failure shall occur locally. Second, this local failure must spread to the rest of the structural elements. Third, the damage extent of the prior initial failure should be disproportional to the final damage state. Caredda et al., (2023) identify various initiators for local damage, including extreme loads such as accidental blasts, intentional explosions by terrorists, design errors, construction errors, improper changes of use, material strength degradation, and lack of maintenance.

Two general approaches, called direct and indirect design methods are proposed for reducing the possibility of progressive collapse (ASCE, 2007; DOC, 2007; DOD, 2009; GSA, 2003). The direct design method formulates a resistance against progressive collapse by providing maximum strength of key structural elements and designing structures that can bridge across the local failure zone. This method applies to buildings in medium and high levels of importance.

On the contrary, the indirect method requires designers to incorporate general structural integrity measures throughout the process of structural system selection, layout of vertical load-bearing elements, member proportioning, and detailing of connections, which then increase the overall robustness of the structure (ASCE, 2007; DOC, 2007; DOD, 2009; GSA, 2003).

In the alternative path method, the structure must possess the capability to bridge over a missing column or bearing by redirecting loads along alternative load paths. According to DOD (DOD, 2009), structural analyses are required to account for the removal of critical load-bearing elements, particularly external columns near the middle of each side, corner, and interior. Marchand et al., (2006) suggests the removal of the column from the structural model is undertaken without degrading the joint's capabilities at the upper end of the member. Physically, the feasibility of this action depends on the type of event causing the damage. Critics often label this form of column removal as immaculate removal. However, it is crucial to note that the alternative load path method is not intended to replicate the actual event; its objective is to verify that the structure exhibits satisfactory flexural resistance to facilitate bridging across an area with limited and localized damage.

Due to the unique nature of various structures, which often feature distinguishing architectural details, establishing a set of progressive collapse analysis considerations applicable to every facility is impractical (GSA, 2003). Some columns in a building may serve primarily architectural functions rather than being true structural columns, introducing uncertainty for the analyst when determining which primary vertical support to remove in the analysis process. To address this knowledge gap, GSA, (2003) recommends and outlines the use of engineering judgment to identify critical analysis scenarios for assessing a structure susceptible to disproportionate collapse. Potential structural configurations leading to atypical arrangements include but are not limited to (a) structures with vertical discontinuities, (b) buildings with structural bays exhibiting significant size variations, and (c) plan irregularities such as re-entrant corners or closely spaced columns.

Numerical investigations into the progressive collapse analysis of buildings employing diverse configurations and modeling techniques were conducted by researchers (Djauhari et al., 2019; Kevins & Tushar, 2017; Khan & Thomas, 2021; Singh et al., 2015). Khan & Thomas, (2021) focused on a step back-set building with secondary columns, analyzing a 12-story RC building with a 4-bay step-back configuration. To enhance structural performance against progressive collapse, secondary columns were strategically placed near exterior columns along the horizontal direction of irregularity. This intervention resulted in a 33.43% reduction in nodal displacement and an 11.39% decrease in the demand capacity ratio (DCR). Kevins & Tushar, (2017) explored the impact of structural irregularity on the progressive collapse of RC buildings with varying story levels (G + 10–G + 30). Utilizing the GSA (GSA, 2003) guideline, the authors applied a single sudden loss of column scenario at four different locations. Their findings suggested that buildings with mass irregularity distributed over multiple stories exhibit less vulnerability compared to those with irregularity confined to a single story.

Moving on to framed RC structures with re-entrant corners, researchers (Djauhari et al., 2019; Gagan & Nayak, 2019; Singh et al., 2015) conducted further numerical investigations. Singh et al., (2015) analyzed a 5-story RC building, following the GSA, (2003) guideline and employing linear static analysis. Although the anticipated DCR values were within permissible limits, the authors overlooked examining column loss at re-entrant corners. Djauhari et al., (2019) studied a ten-story RC building with 3.6 m story floor levels, finding

a maximum DCR of 3.443 and a domino-type failure mode for an atypical building. Gagan & Nayak, (2019), studying a 12-story RC building, deviated from the GSA, (2003) guideline by employing linear static analysis. Their research yielded different DCR values for various seismic zones.

Vertical irregularity studies were extended by researchers (Haq & Agarwal, 2019; Kazem et al., 2012). Haq & Agarwal, (2019) examined three 20-story RC framed buildings with and without atrium, stepped along the shorter span. They concluded that high-rise RC frame structures exhibit greater tendencies to redistribute moments after collapse, offering increased resistance against disproportionate collapse. The authors recommended further studies exploring the effects of different bay sizes, atrium space, and unforeseen irregularities.

Kazem et al., (2012) assessed the progressive collapse resistance of reinforced concrete buildings with irregularities in height. Their numerical analysis revealed that for asymmetric structures in height, the level of deduction in the increment of energy absorption ability varied, necessitating additional redundancy.

Sustainability assessments of the progressive collapse of RC flat slab buildings were conducted by researchers (Garg et al., 2020a, 2020b, 2021a, 2021b). Focusing on a 3×5 bays regular framed building with and without perimeter beams, the authors (Garg et al., 2020b) utilized the equivalent frame method and linear static analysis in alignment with GSA (GSA, 2003) acceptance criteria. The study examined the sudden loss of columns from a five-story RC flat building using linear static analysis, emphasizing the use of perimeter beams to strengthen the proposed structural configuration.

Furthermore, Sujeevan & Kurminaidu, (2017) explored the progressive collapse of a ten-story RC building designed for various seismic zones. The authors concluded that linear-static analysis can provide reasonable results with reduced computational time and cost, aligning with conclusions reached by other researchers (Garg et al., 2020a, 2020b, 2021a, 2021b). Obeng Ankmah et al., (2018), focusing on the linear-static analysis approach, asserted that the dynamic load increase factor proposed by GSA (GSA, 2003) is conservative, a viewpoint also supported by similar findings presented by Esfandiari et al. (Esfandiari & Urgessa, 2020; Esfandiari et al., 2023; Esfandiari et al., 2018).

Most research on progressive collapse focuses on symmetrical structural configurations and limited irregularity schemes. Additionally, the majority of reviewed literature overlooks the impact of actions stemming from solid slab and shear wall systems. To address this knowledge gap, this paper explores the progressive collapse of both typical and three atypical structural configurations, each incorporating a solid slab and shear wall system. The three atypical configurations, absent from the reviewed literature, include an RC framed building with a re-entrant corner side (ATYP_FRM1), a 12° vertically tilted framed building (ATYP_FRM2), and an RC framed building with closely-spaced columns (ATYP_FRM3), all accompanied by a solid slab floor system and shear wall. The study adheres to conventional design and detailing standards for all framed structural configurations in accordance with EN (EN, 2002).

2 Details of the Numerical Models

According to GSA, (2003), dynamic effects can be taken into consideration in different ways depending on the analytical technique selected. One way of inducing the dynamic effect is the consideration of dynamic increase factors (DIF) in the material properties. In this paper, as supported by the GSA, (2003), the linear-static method of structural analysis accompanied by DIFs on which the dynamic amplifiers simulate and account for the sudden loss of column and strength enhancement due to the strain rate were employed.

2.1 Material Property

The material properties used in this paper are summarized in Table 1. According to Sect. 4.1.2.5 of GSA, (2003), a dynamic increase factor of 1.25 was used for both the compressive strength of concrete and the tensile strength of reinforcement steel bars. Thus, all the structural elements in this study were analyzed and designed by using a material property listed in Table 1.

2.2 Geometric Property

The study considered eight-story 24 m high buildings that were designed and detailed following the EN, (2002) for an office occupancy. Figure 1 presents the building layouts. The story height in each building is 3 m. All columns were fixed against translational and rotational degrees of freedom. The typical structural configuration (TYP_FRM) considered in this study had a regular layout of a 25 m x 19 m planar area. In contrast, atypical structural configurations with re-entrant corner side (ATYP_FRM1), 12° vertically tilted structural layouts (ATYP_FRM2), and closely-spaced columns (ATYP_FRM3) were proposed to represent irregular layouts. The nature and classification of atypical structural configuration was made following GSA, (2003) Appendix-A. From the aforementioned atypical structural configurations, it is evident that the possible structural configurations were deployed to include variations in bay size, plan irregularity, and closely spaced columns. Despite the similarity in material strength parameters, all typical and atypical structural

Table 1 Mechanical properties of material EN (EN, 2002)

Mechanical property	Material	Value
Mean density (kg/m^3)	Concrete	2500
	Reinforcing steel	7850
Characteristics cylindrical compressive strength of concrete (MPa)		25
Cube compressive strength of concrete (MPa)		30
Characteristics yield strength of reinforcing steel (MPa)		420
Ultimate tensile strength of reinforcing steel (MPa)		600
Elastic modulus (GPa)	Concrete	31
	Reinforcing steel	200
Linear coefficient of thermal expansion (1/C°)	Concrete	10×10^{-6}
	Reinforcing steel	10.1×10^{-6}
Poisson ratio	Concrete	0.2
	Reinforcing steel	0.3

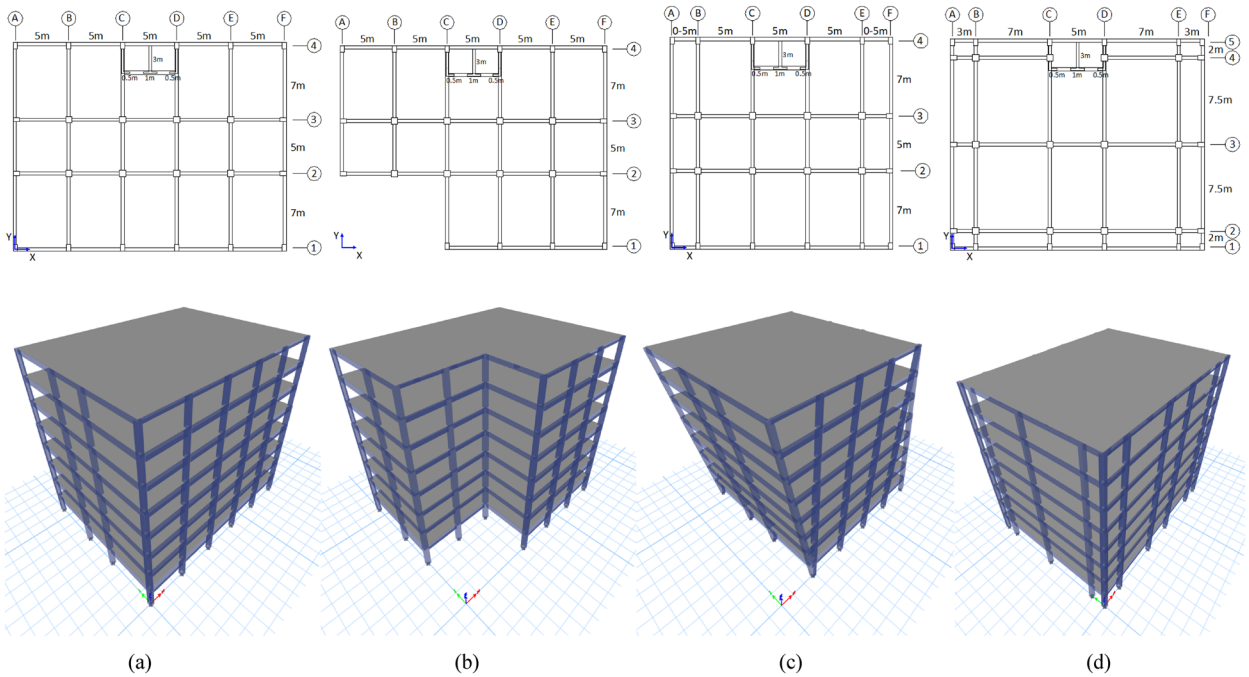

Fig. 1 Plan and 3D view of frames: **a** TYP_FRM; **b** ATYP_FRM1; **c** ATYP_FRM2; and **d** ATYP_FRM3

configurations are designed to have different sectional properties and reinforcing steel details (see Tables 2, 3, 4 and 5).

For both typical and atypical structural configurations, the roof and typical floor slabs were designed to have 120 mm and 150 mm thickness respectively. Consequently, the reinforced concrete wall designed to carry the lift shafts had 140 mm thickness. When considering floor loads, the live and dead loads for the typical floors 1–7th were 5 kN/m^2 and 20 kN/m^2 respectively. On the other hand, the dead and live on the roof floor (8th story) were computed to be 5 kN/m^2.

2.3 Method of Analysis

2.3.1 Linear Static Analysis

For buildings with a height of 10 stories or less, GSA, (2003) recommends the application of the alternate load path method to evaluate the susceptibility of both new and existing structures to progressive collapse. This prescriptive structural analysis method

Table 2 Geometrical and reinforcing steel detail for TYP_FRM

Beam					
Story	**Axis**	**Cross-sectional dimension**	**Longitudinal reinforcing steel**		**Stirrup**
			Compression bar	**Tension bar**	
8th	X	250 mm x 300 mm	3φ20 mm	4φ20 mm	φ8@150 mm
	Y	250 mm x 450 mm	3φ20 mm	4φ20 mm	φ8@150 mm
1st–7th	X &Y	350 mm x 500 mm	4φ20 mm	5φ20 mm	φ8@100 mm
Column					
Grid: 1A, 1B, 1C, 1D, 1E, 1F, 2A, 2F, 3A, 3F, 4A, 4B, 4C, 4D, 4E & 4F					
Story		**Cross-sectional dimension**	**Longitudinal reinforcement**		**Tie**
1st–5th		500 mm x 600 mm	10φ20 mm		φ8@150 mm
6th–8th		400 mm x 500 mm	10φ20 mm		φ8@200 mm
Grid: 2B, 2C, 2D, 2E, 3B, 3C, 3D, & 3E					
1st–5th		600 mm x 600 mm	8φ28 mm		φ8@150 mm
6th–8th		500 mm x 500 mm	8φ28 mm		φ8@200 mm

Table 3 Geometrical and reinforcing steel detail for ATYP_FRM1

Beam					
Story	**Axis**	**Cross-sectional dimension**	**Longitudinal reinforcing steel**		**Stirrup**
			Compression bar	**Tension bar**	
8th	X	250 mm x 300 mm	3φ20 mm	4φ20 mm	φ8@150 mm
	Y	250 mm x 450 mm	3φ20 mm	4φ20 mm	φ8@150 mm
1st–7th	X &Y	350 mm x 500 mm	4φ20 mm	5φ20 mm	φ8@100 mm
Column					
Grid: 1C, 1D, 1E, 1F, 2A, 2F, 3A, 3F, 4A, 4B, 4C, 4D, 4E & 4F					
Story		**Cross-sectional dimension**	**Longitudinal reinforcement**		**Tie**
1st–5th		500 mm x 600 mm	10φ20 mm		φ8@150 mm
6th–8th		400 mm x 500 mm	10φ20 mm		φ8@200 mm
Grid: 2B, 2C, 2D, 2E, 3B, 3C, 3D, & 3E					
1st–5th		600 mm x 600 mm	8φ28 mm		φ8@150 mm
6th–8th		500 mm x 500 mm	8φ28 mm		φ8@200 mm

necessitates and provides the analyst with the ability to examine the vulnerability and performance of a structural framework when subjected to disproportionate collapse. Furthermore, as outlined in GSA, (2003), the linear static analysis approach can be employed to appraise the potential for progressive collapse in all newly constructed facilities. The procedure involves a static linear elastic approach, specifying criteria for analyzing results, a set of analysis cases, and loading criteria tailored for the analysis. The analytical procedures that could be used for the alternate load method accompanied by the linear static method are presented as follows.

For the linear static analysis, GSA, (2003) recommends the use of amplification factors also known as dynamic increase factors, and 3-dimensional models be used to account for potential 3-dimensional effects and avoid overly conservative solutions. By doing so, the linear static analysis enables the engineer to determine the critical situations that should be assessed for the potential for progressive collapse with less computational

Table 4 Geometrical and reinforcing steel detail for ATYP_FRM2

Beam					
Story	**Axis**	**Cross-sectional dimension**	**Longitudinal reinforcing steel**		**Stirrup**
			Compression bar	**Tension bar**	
8th	X	250 mm x 300 mm	3φ20 mm	4φ20 mm	φ8@150 mm
	Y	250 mm x 450 mm	3φ20 mm	4φ20 mm	φ8@150 mm
1st–7th	X &Y	350 mm x 500 mm	4φ20 mm	5φ20 mm	φ8@100 mm
Column					
Grid: 1A, 1B, 1C, 1D, 1E, 1F, 2A, 2F, 3A, 3F, 4A, 4B, 4C, 4D, 4E & 4F					
Story		**Cross-sectional dimension**	**Longitudinal reinforcement**		**Tie**
1st–5th		500 mm x 600 mm	10φ20 mm		φ8@150 mm
6th–8th		400 mm x 500 mm	10φ20 mm		φ8@200 mm
Grid: 2B, 2C, 2D, 2E, 3B, 3C, 3D, & 3E					
1st–5th		600 mm x 600 mm	8φ28 mm		φ8@150 mm
6th–8th		500 mm x 500 mm	8φ28 mm		φ8@200 mm

Table 5 Geometrical and reinforcing steel detail for ATYP_FRM3

Beam					
Story	**Axis**	**Cross-sectional dimension**	**Longitudinal reinforcing steel**		**Stirrup**
			Compression bar	**Tension bar**	
8th	X	250 mm x 300 mm	3φ20 mm	4φ20 mm	φ8@150 mm
	Y	250 mm x 450 mm	3φ20 mm	4φ20 mm	φ8@150 mm
1st–7th	X &Y	350 mm x 500 mm	4φ20 mm	5φ20 mm	φ8@100 mm
Column					
Grid: 1A, 1B, 1C, 1D, 1E, 1F, 2A, 2F, 3A, 3F, 4A, 4F, 5A, 5B, 5C, 5D, 5E & 5F					
Story		**Cross-sectional dimension**	**Longitudinal reinforcement**		**Tie**
1st–5th		500 mm x 600 mm	10φ20 mm		φ8@150 mm
6th–8th		400 mm x 500 mm	10φ20 mm		φ8@200 mm
Grid: 2B, 2C, 2D, 2E, 3B, 3C, 3D, 3E, 4B, 4C, 4D, & 4E					
1st–5th		600 mm x 600 mm	8φ28 mm		φ8@150 mm
6th–8th		500 mm x 500 mm	8φ28 mm		φ8@200 mm

time and cost. Thus, in the present study, a 3D model comprising both RC slab and shear wall system was modeled by using the ETABS software. The alternative load path mechanism and the demand-capacity ratio (DCR) acceptance criteria, which are usually extracted and used to evaluate the assessment of the potential for progressive collapse of buildings were used. As detailed in GSA, (2003) Sect. 4.1.2.4, following the linear static analysis, a DCR is computed for each of the structural members in a building as shown in Eq. 1.

$$DCR = \frac{Qd}{Qc} \tag{1}$$

where, Q_d = Demand (moment, axial force, shear force, or combined actions) post-processed from the linear-static analysis. Q_c = Capacity of the member (moment, axial force, shear force, or combined actions) that the member can resist.

Following GSA (GSA, 2003), Sect. 4.1.2.4, Eq. 4.2 expresses the acting and expected ultimate forces (Q_d and Q_c) in terms of moment, axial force, shear force, or

combined P-M2-M3 values. Additionally, in the analysis, to account for the strength enhancement conditions of a material when subjected to disproportionate collapse, the design material strength is augmented by a dynamic increase factor (DIF).

Therefore, this study considered the combined P-M2-M3 actions, typically computed using the ETABS FEA packaged program. The dimensionless demand capacity ratio (DCR) of Q_d and Q_c was computed, traced, and extracted from the post-processed files of the program. Additionally, GSA, (2003) anticipates that building structural elements and beam-column connections with typical and atypical structural configurations, having a DCR greater than 2.0 and 1.5, respectively, can be considered as having a high potential for progressive collapse. In other words, a member is classified as failed if its DCR at any section satisfies the following conditions:

DCR $\geq$ 2.0; for typical (regular) building.

DCR $\geq$ 1.5; for atypical (irregular) buildings.

The demand capacity ratio (DCR) was calculated from the combined P-M2-M3 action interaction surfaces, also known as coupled actions. These surfaces are based on the interaction of axial force and bi-axial bending moments at the hinge location. Since all the analysis models were 3D, a three-dimensional P-M2-M3 space was considered to capture yielding occurrences for different combinations of axial force (P), minor moment (M2), and major moment (M3).

To establish the demand and capacity ratios, the points on the curves were ordered from the most negative (compressive) value of P to the most positive (tensile). The baseline of the first point of all curves shared identical values of P, M2, and M3. Additionally, the curves were defined in a counter-clockwise direction when viewed from above (looking toward compression), and the surface appeared convex, ensuring that the tangent planes at any point were entirely outside the surface. However, any points that were "pushed in" were automatically adjusted by the program to maintain tangent planes outside the surface. A warning would be issued during analysis if a non-convex surface was encountered.

2.3.2 Column Removal Scenarios

The speed at which an element is removed has no impact on a static analysis GSA, (2003). In this study, the alternative load path mechanism was deployed and the column that is removed was removed instantaneously. The rationale for the sudden removal of columns initiated at the first and fifth stories of the building was evaluated following GSA, (2003) Sect. 5.1.2.3. Following the provisions of GSA, (2003) Sect. 5.1.2.3, four possible column removal scenarios, each with only one column removed at a time, were considered. As shown in Fig. 2, for both typical and atypical structural configurations, the first column (C1) removal was located on the perimeter, approximately in the middle of the long side of the building. The second column (C2) was removed from the perimeter of the building specifically on the middle of the short side. The third sudden column (C3) removal location was located at the corner (re-entrant) side of the buildings and for both structural configurations, the probable location for interior column (C4) was coordinated from the mid-point located inside the planar area of the floor system.

In this study, the following steps were undertaken:

1 Design and detailing of space models for both typical and atypical framed structural configurations were performed following (EN).
2 Linear static analysis was applied, incorporating material strength enhancement factors.
3 Four distinct scenarios of sudden column loss were simulated, with one column loss per analysis.
4 Disproportionate Collapse Ratio (DCR) values were derived from the program's beam, column, and beam-column joint P-M2-M3 interaction analysis module.
5 These values were subsequently illustrated on the corresponding members, initiating a discussion on the vulnerability of each member to progressive collapse.

3 Results and Discussion

The maximum combined action (P-M2-M3) demand capacity ratio (DCR) values for primary structural components (beams, columns, and beam-column joints) on both X and Y axes were extracted. As discussed in Sect. 2.3.1, the combined P-M2-M3 actions, also referred to as coupled actions, are based on the interaction of axial force and bi-axial bending moments at the hinge location. For easier visualization, beams and columns that exceeded the DCR limit are designated in red color and they have a high potential for progressive collapse.

3.1 Column Removed from Middle Side of the Long Axis

Figures 3, 4, 5 and 6 shows the DCR values for TYP_FRM, ATYP_FRM1, ATYP_FRM2, and ATYP_FRM3 structural configurations along with the longitudinal and transverse frame of the removed column C1. From the figures, on the TYP_FRM, with respect to the first story column loss case, a total of 20 beams on the first story along X-and Y-axis had exceeded the DCR limit provided by GSA, (2003). In contrary to this, on column loss at the fifth story scenario, only 1 beam had exceeded the limit. On the other hand, for atypical frame layout with re-entrant corner (ATYP_FRM1), considering the X-axis, 14

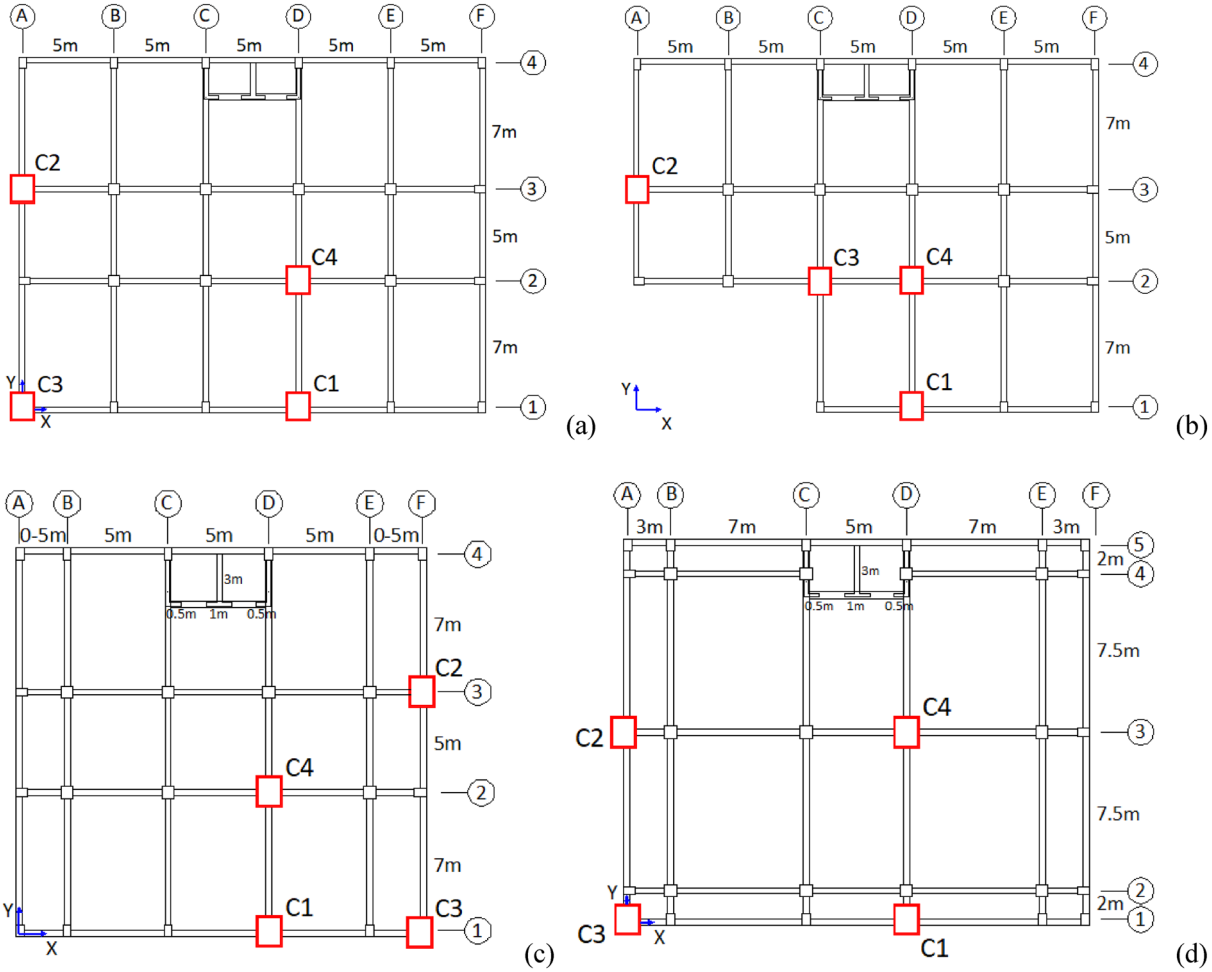

Fig. 2 Sudden column removal locations: **a** TYP_FRM; **b** ATYP_FRM1; **c** ATYP_FRM2; and **d** ATYP_FRM3

beams & 4 columns and 6 beams & 4 columns on the first and fifth story column loss scenarios, respectively, had exceeded the DCR limit. While so, for the same structural system (ATYP_FRM1), a total of 16 beams in both X and Y axes resulted a DCR value greater than 1.5. Likewise, for atypical frame layout with 12° inclined frame (ATYP_FRM2), 14 beams & 5 columns and 6 beams & 3 columns in X-axis, on the first and fifth story column loss scenarios, respectively, had exceeded the 1.5 limit. While so, for ATYP_FRM2 structural configuration, a total of 16 beams in both X and Y had exceeded the DCR limit. Likewise, for atypical frame layout with closely spaced columns (ATYP_FRM3), considering only Y-axis, 18 beams & 5 columns and 15 beams & 2 columns on the first and fifth story column loss scenarios, respectively, had exceeded the DCR limit.

Thus, it is evident that the DCR values for beams with short spans, which are stiffer than the long-span beams, attracted larger demands (P-M2-M3 combined actions). Therefore, the resulting endpoints adjoining short span beams had a high potential for progressive collapse. Moreover, comparing the sudden loss of a column on the first story with the fifth story, the DCR values are larger for the former case causing it to be more vulnerable to progressive collapse.

Figure 7 presents the maximum DCR values for the typical (TYP_FRM) and atypical (ATYP_FRM1, 2 & 3) structural configuration story levels. It is evident that ATYP_FRM3 had the maximum DCR values for both progressive collapse scenarios.

3.2 Column Removed from Middle Side of the Short Axis

Figures 8, 9, 10 and 11 show the DCR values for TYP_FRM, ATYP_FRM1, ATYP_FRM2, and ATYP_FRM3 structural configurations along with the longitudinal and transverse frame of the removed column C2. From the figures, for both first and fifth story column loss cases on the TYP_FRM layout along X axis, a total of 8 beams,

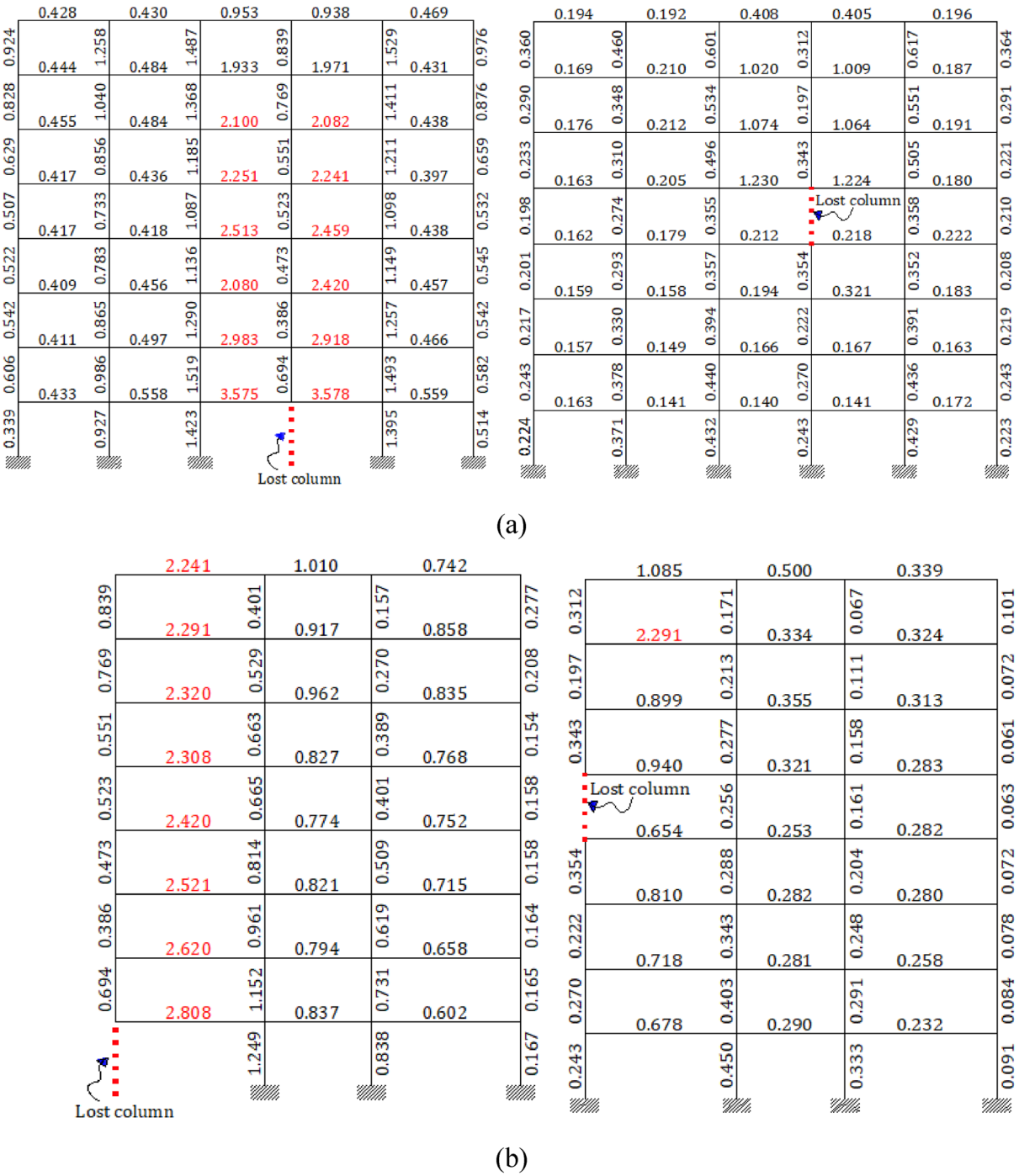

Fig. 3 DCR values for TYP_FRM column C1 removal scenario on 1st and 5th story: **a** X-axis; **b** Y-axis

respectively, exceeded the DCR limit provided by GSA, (2003). The same result was obtained for Y-axis. Likewise, for atypical frame layout with re-entrant corner (ATYP_FRM1), considering the first floor column loss along X and Y-axes, a total of 16 beams were found to be vulnerable to damage caused by progressive collapse. The same result was obtained for the fifth floor column loss case along X and Y-axes. Conversely, considering TYP_FRM2 when accompanied by column loss at the first story scenario, only 1 beam had exceeded the DCR limit (1.5). Exclusively, for atypical frame layout with closely spaced columns (ATYP_FRM3), considering only X-axis, 22

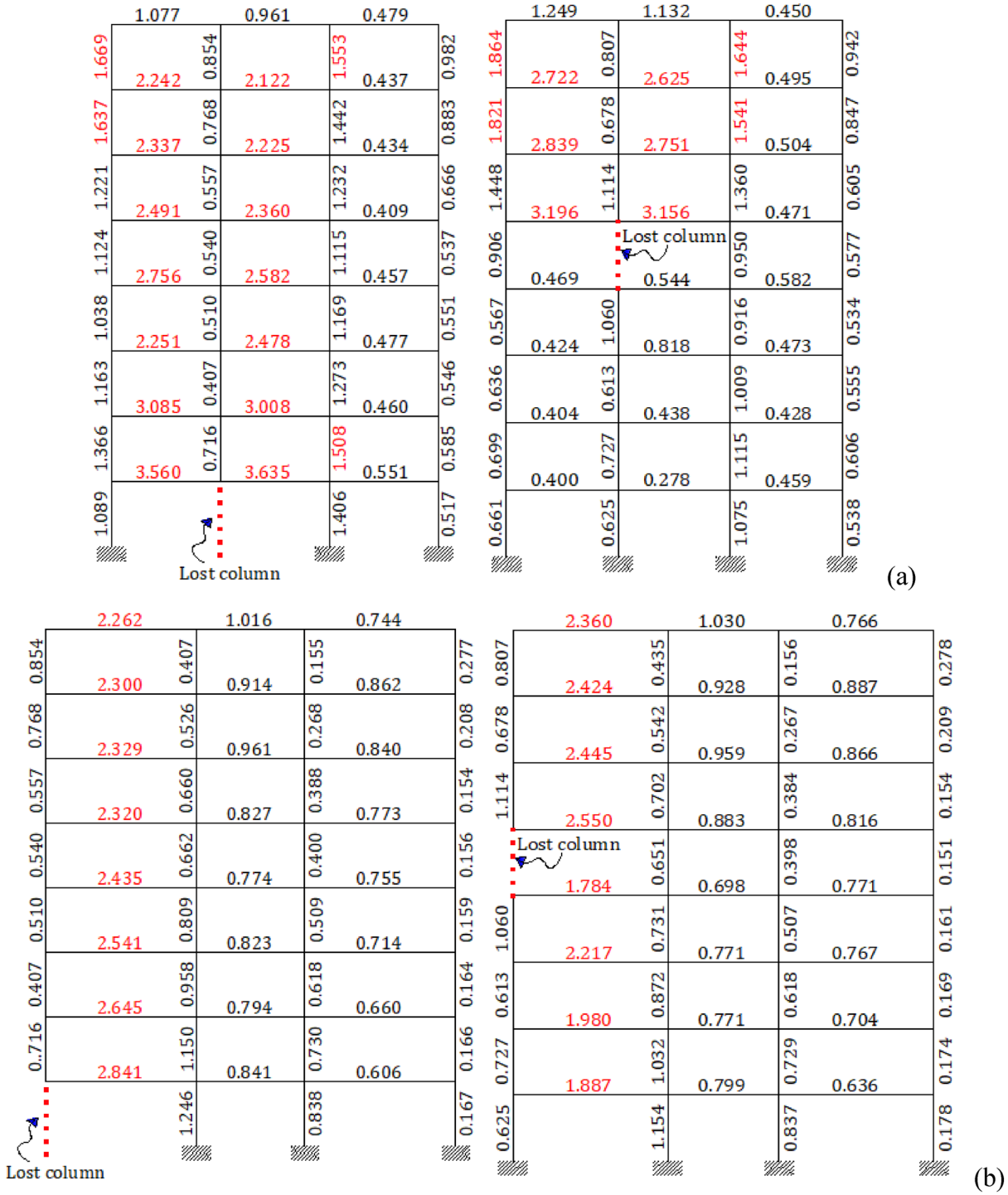

Fig. 4 DCR values for ATYP_FRM1 column C1 removal scenario on 1st and 5th story: **a** X; **b** Y-axis

beams & 10 columns and 16 beams & 11 columns on the first and fifth story column loss scenarios, respectively, were found to be highly vulnerable to damage caused by progressive collapse. Thus, it can be anticipated that the DCR values for beams with short spans, which are stiffer than the long-span beams, attract larger demands (P-M2-M3 combined actions).

Figure 12 presents the maximum DCR values for the typical (TYP_FRM) and atypical (ATYP_FRM1, ATYP_FRM2 & 3) structural configuration story levels. In

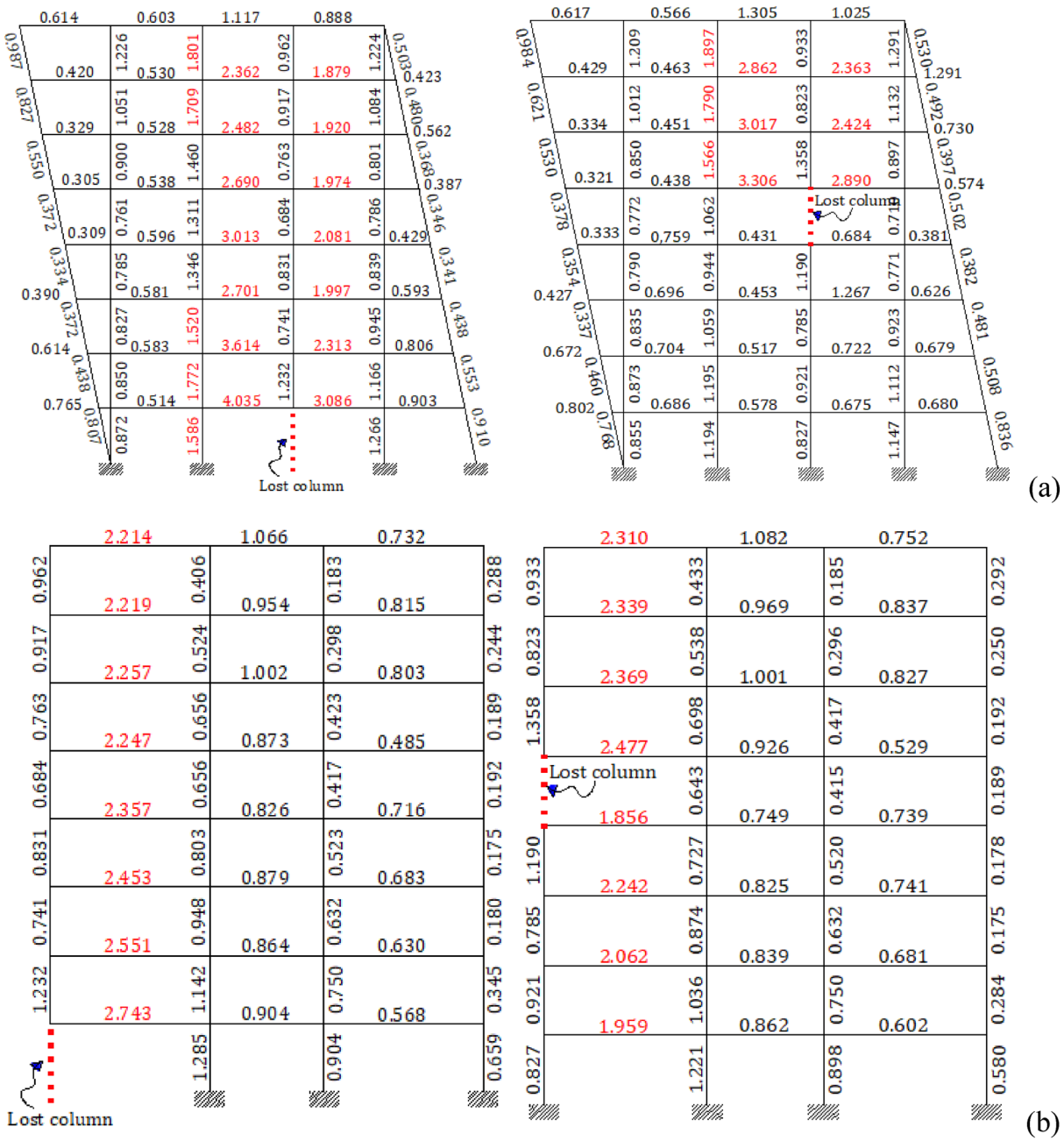

Fig. 5 DCR values for ATYP_FRM2 column C1 removal scenario on 1st and 5th story: **a** X; **b** Y-axis

comparison, ATYP_FRM3 has the maximum DCR values with the highest exposure to progressive collapse.

3.3 Column Removed from the Re-entrant Corner

Figures 13, 14, 15 and 16 show the DCR values for TYP_FRM, ATYP_FRM1, ATYP_FRM2, and ATYP_FRM3 structural configurations along with the longitudinal and transverse frame of the removed column C3. For atypical frame layout with re-entrant corner (ATYP_FRM1), considering both X and Y-axes, column loss at the first story revealed the high vulnerability of 31 beams to damage caused by progressive collapse. Whereas, on the Y-axis both column loss cases on the fifth story revealed a damage of 24 total number of beams. For both sudden column loss at the first and fifth story, only one beam failed in TYP_FRM and for ATYP_FRM2 & 3, no primary structural member has exceeded the DCR limit. For the proposed sudden column loss location, the contribution

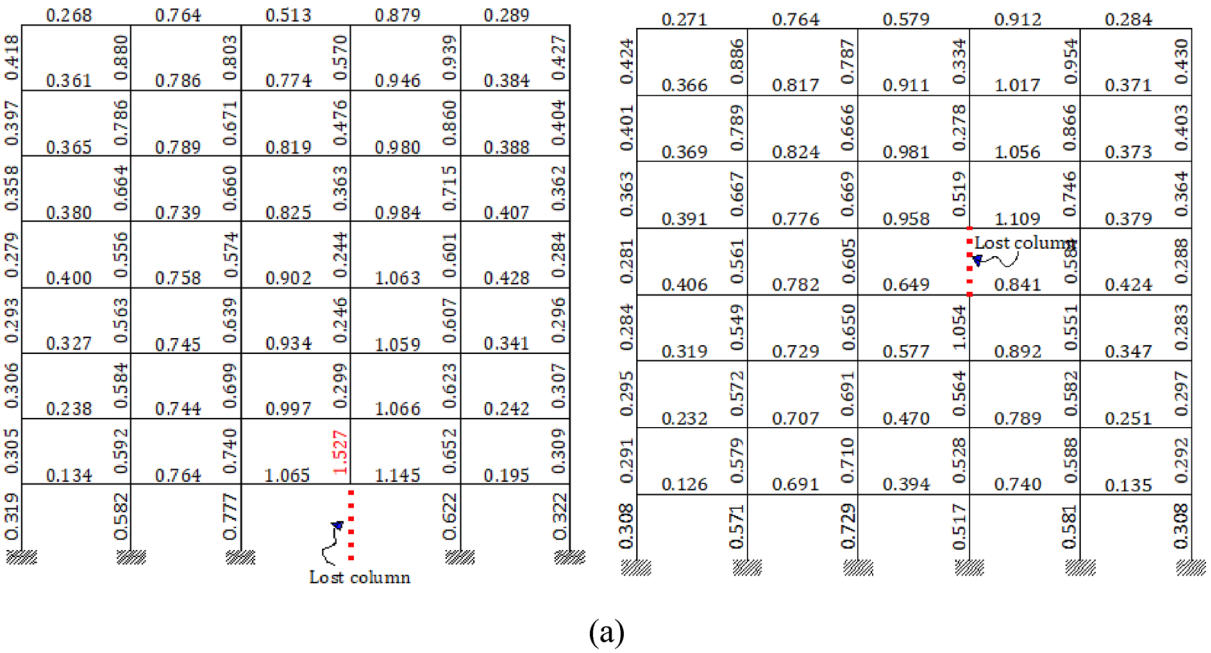

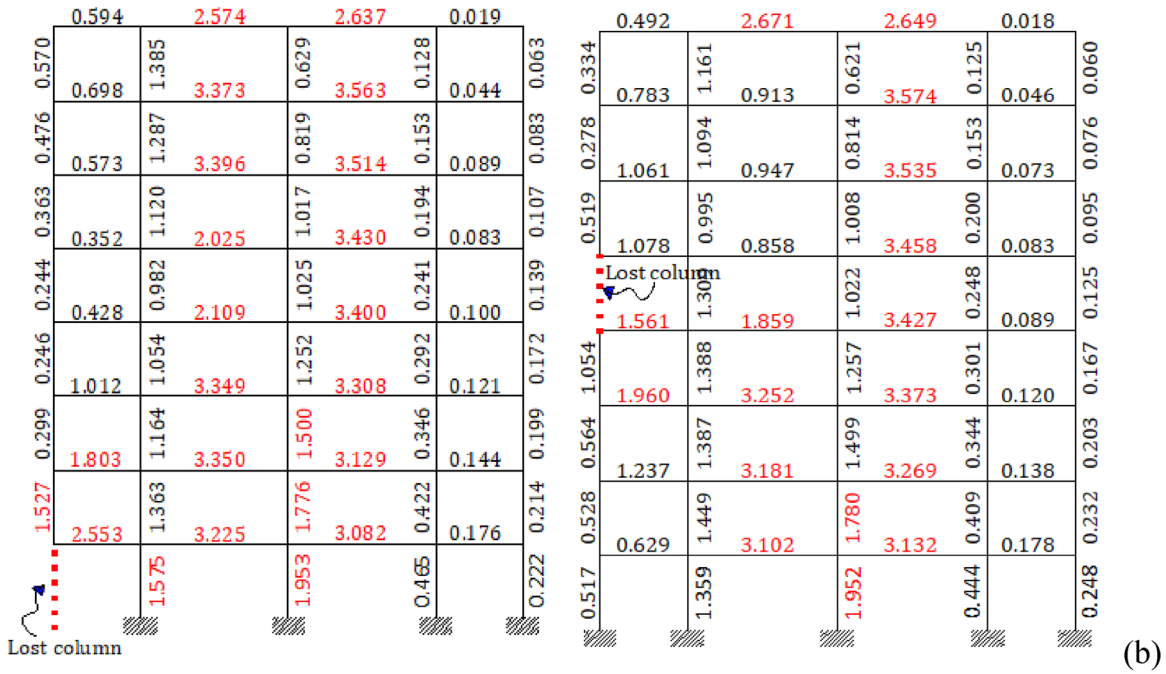

Fig. 6 DCR values for ATYP_FRM3 column C1 removal scenario on 1st and 5th story: **a** X; **b** Y-axis

from better alternative load path mechanism, the low tributary loaded floor area and nature of the structural connectivity were rendered to make ATYP_FRM2 & 3 provide robustness against progressive collapse. In contrast, for a sudden loss of column at the re-entrant corner (ATYP_FRM1), a high potential for progressive collapse was observed.

Figure 17 depicts the DCR values for beams and columns that exceeded the DCR limit. Thus, after extracting the DCR for all grids along the X and Y axis, for

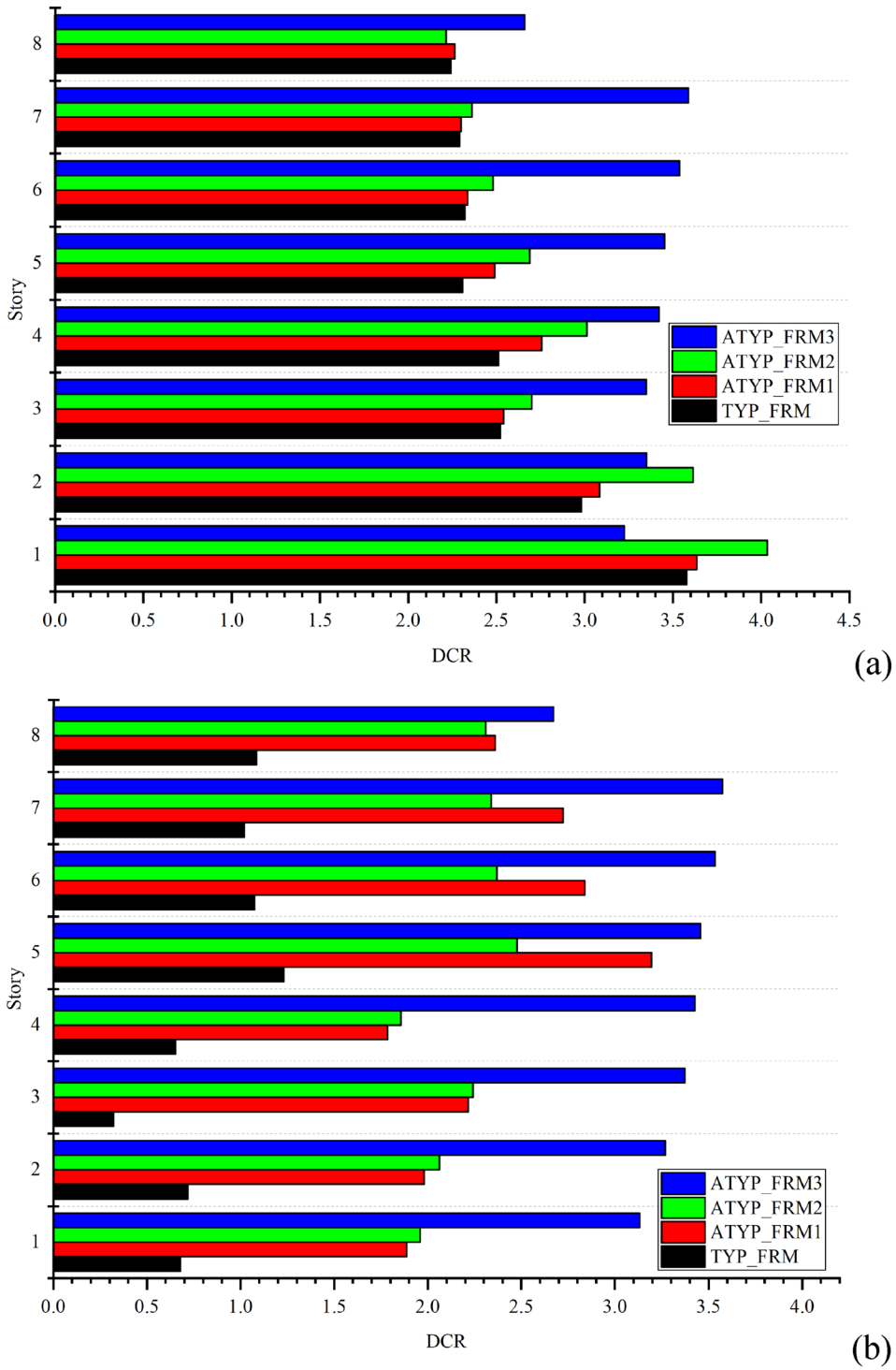

Fig. 7 Comparison of Story vs DCR for column C1 removal scenario case: **a** 1st story; **b** 5th story

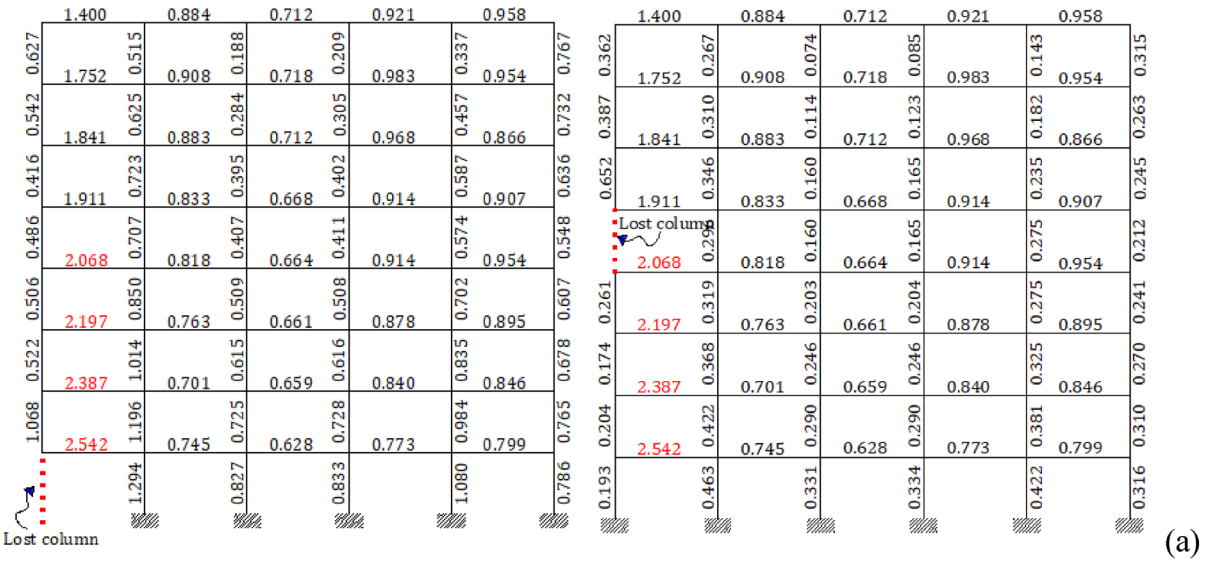

Fig. 8 DCR values for TYP_FRM column C2 removal scenario on 1st and 5th story: **a** X; **b** Y-axis

the sudden column loss at the first story and fifth story, ATYP_FRM3 and ATYP_FRM1 showed larger percentage values respectively.

3.4 Column Removed from the Interior Side

Figures 18, 19, 20 and 21 show the DCR values for TYP_FRM, ATYP_FRM1, ATYP_FRM2, and ATYP_FRM3 structural configurations along with the longitudinal and transverse frame of the removed column C4. From the figures, for TYP_FRM scheme accompanied by the first story column loss case, a total of 31 beams on the first story along X-and Y-axis had exceeded the DCR limit provided by GSA, (2003). On the other hand, on column loss at the fifth story scenario, a total of 16 beams had also exceeded the limit (2.0). On the other hand, for atypical frame layout with re-entrant corner

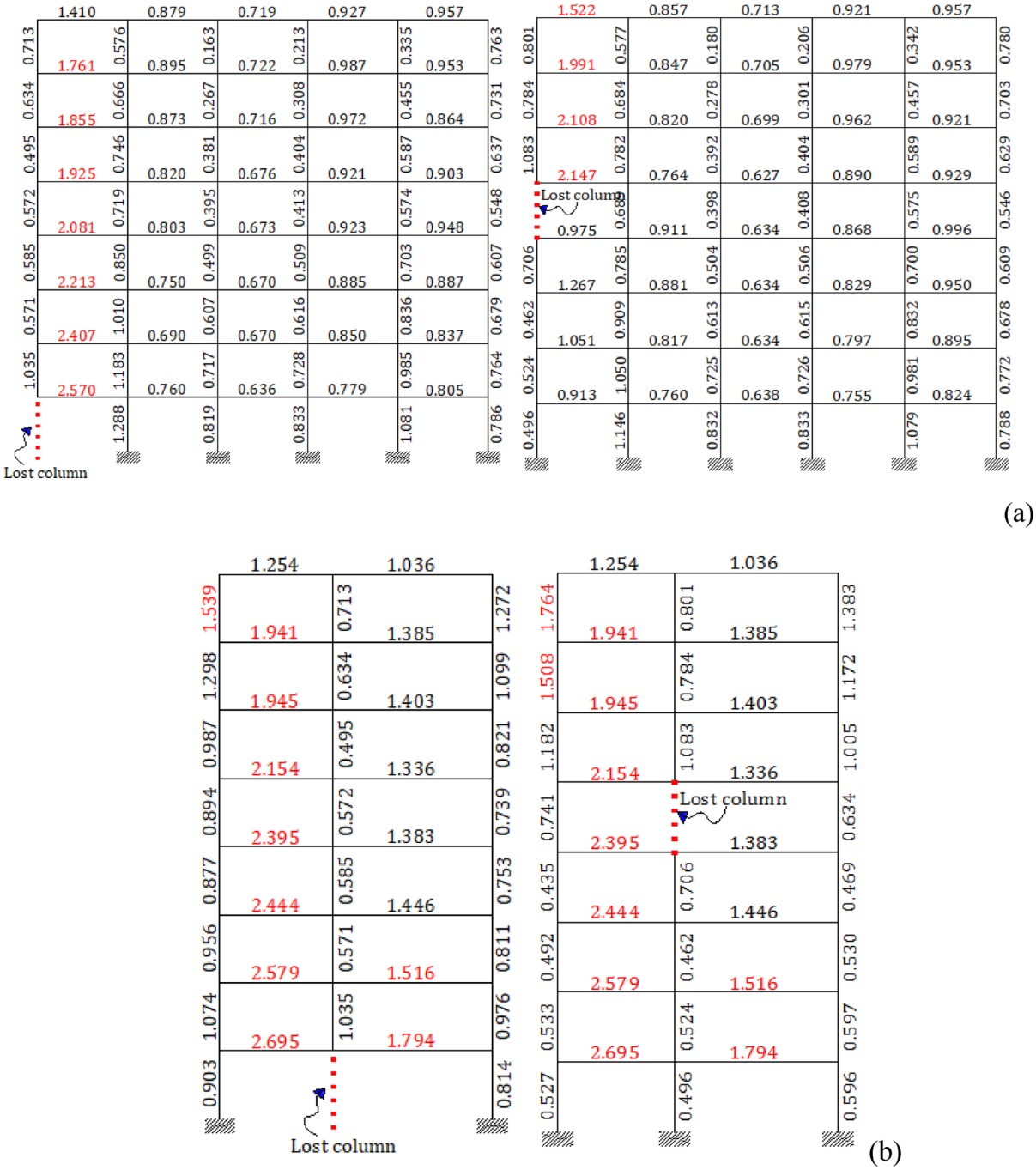

Fig. 9 DCR values for ATYP_FRM1 column C2 removal scenario on 1st and 5th story: **a** X; **b** Y-axis

(ATYP_FRM1), considering the X-axis, on the first and fifth story column loss scenario, a total of 24 beams were found to be vulnerable to disproportionate collapse, respectively. Whereas, considering the Y-axis, for the same structural configuration (ATYP_FRM1), sudden loss of column on the first story yielded a loss of total of 16 beams and 2 columns. Likewise, for the same frame but with column loss at the fifth story, 12 beams and 2 columns had exceeded the DCR limit (1.5).

On the other hand, for atypical frame layout with 12° inclined frame (ATYP_FRM2), considering the X and Y-axis on the first story column loss scenario, a total of 32

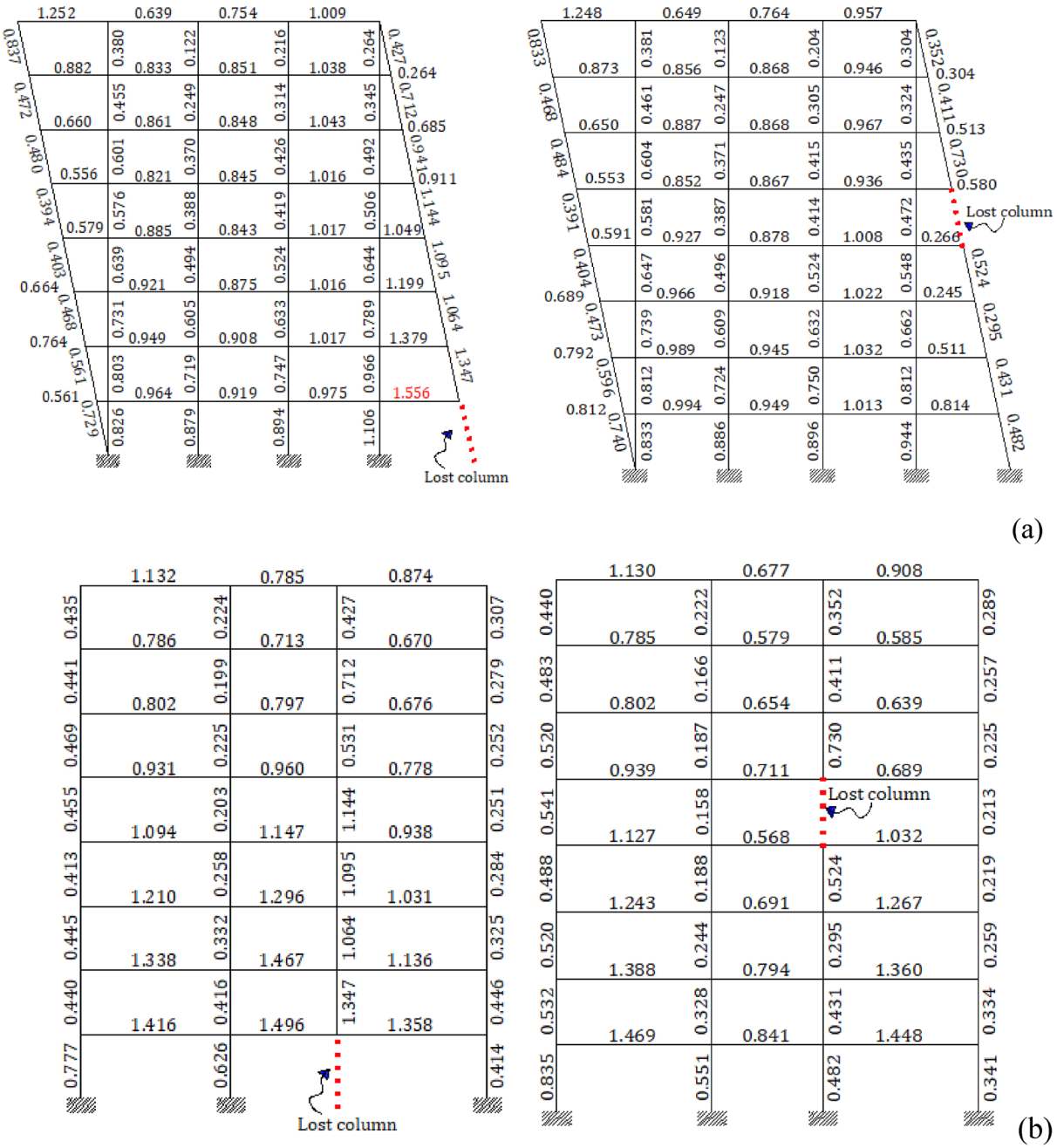

Fig. 10 DCR values for ATYP_FRM2 column C2 removal scenario on 1st and 5th story: **a** X; **b** Y-axis

beams were found to be vulnerable to disproportionate collapse. The same result was obtained for a column loss at the fifth story. Whereas, considering the Y-axis, for the same structural configuration (ATYP_FRM2), sudden loss of column on the first story yielded a loss of 8 beams. Likewise, for the same frame but with column loss at the fifth story, 12 beams and 3 columns were found vulnerable to progressive collapse.

Exclusively, for atypical frame layout with closely spaced columns (ATYP_FRM3), considering a column loss at the first story along X and Y-axis, a total of 42 beams and 29 columns exceeded GSA's, (2003) allowable limit (1.5). Consequently, the same trend was observed for the fifth floor column loss scenario. Considering both the X and Y-axes, a total of 29 beams and

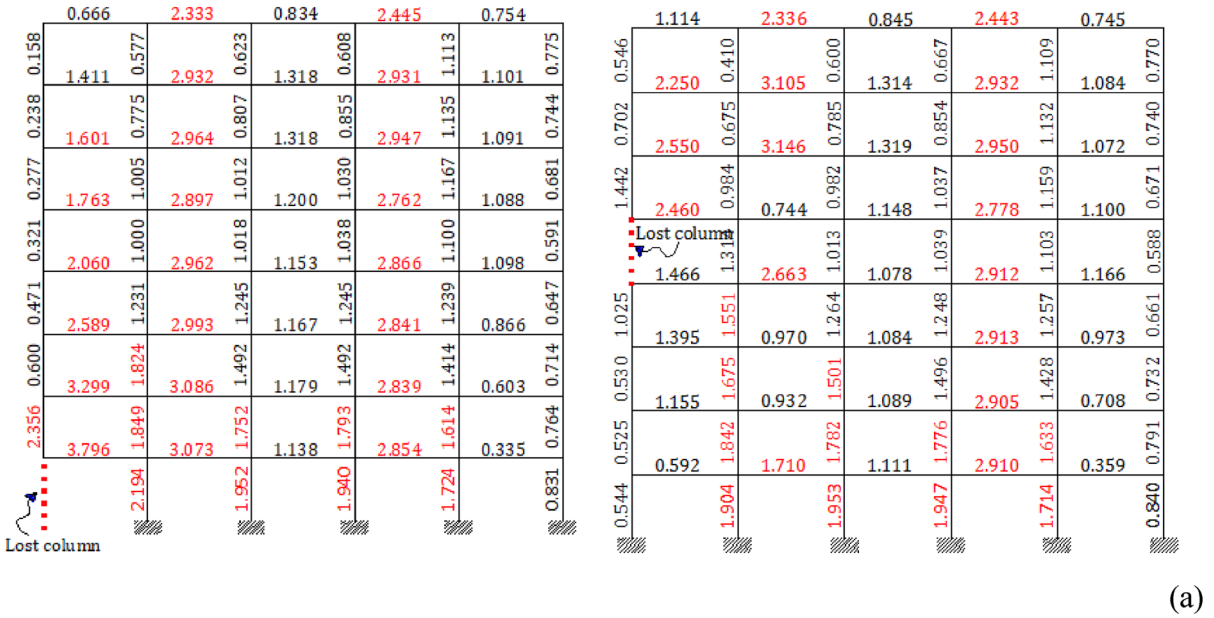

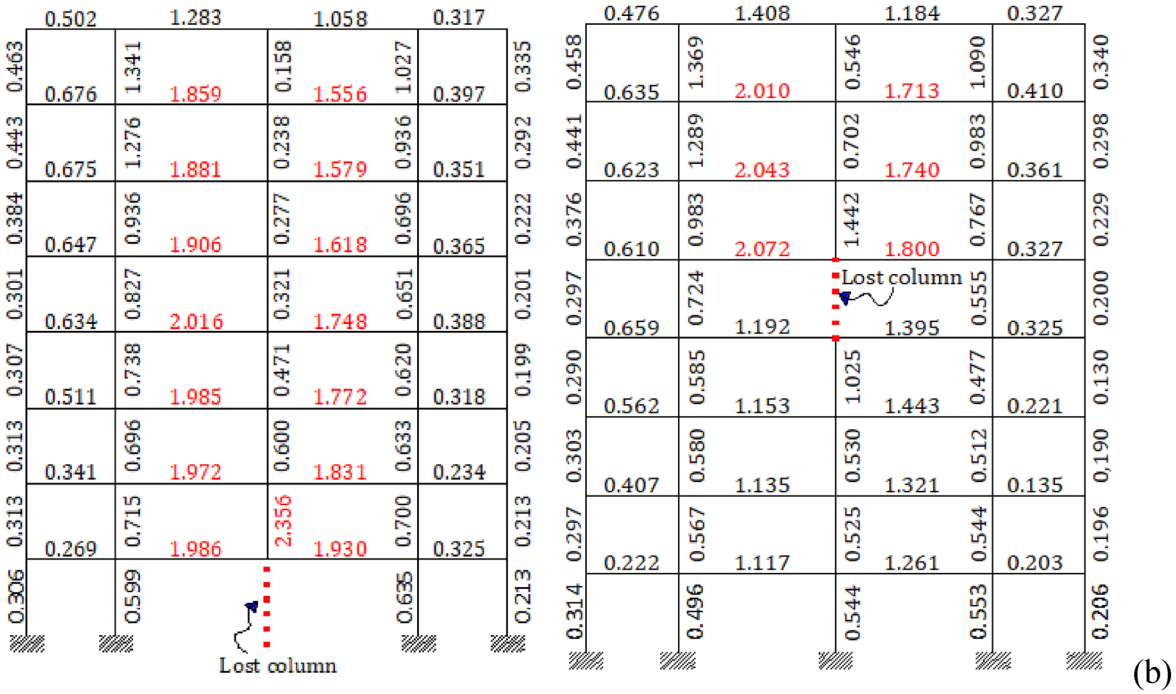

Fig. 11 DCR values for ATYP_FRM3 column C2 removal scenario on 1st and 5th story: **a** X; **b** Y-axis

23 columns were found to be vulnerable to the damage caused by disproportionate collapse.

From the above result, it was insisted that this extensive damage was rendered to be sourced from the larger tributary loaded floor area. Moreover, as seen from the previous sections, members with short span on both longitudinal and transverse frames had a shear failure mode and attracted larger DCR values with significantly increased exposure to progressive collapse.

Among the available total number of primary structural members in TYP_FRM, ATYP_FRM1, ATYP_FRM2, and ATYP_FRM3 structural configurations, the framed structure with closely spaced columns (ATYP_FRM3) has the largest percentage of beams and columns

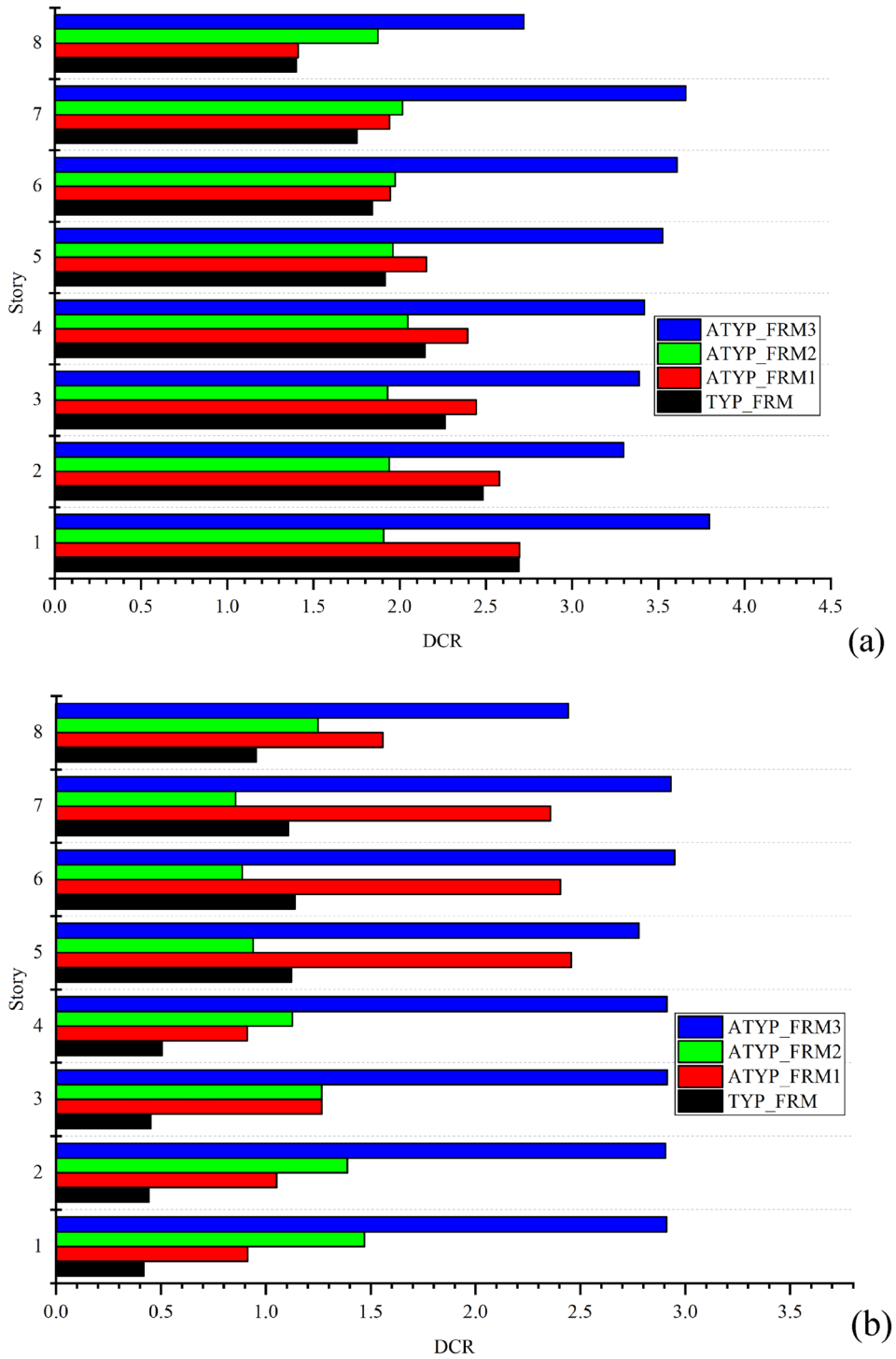

Fig. 12 Comparison of Story vs DCR for column C2 removal scenario case: **a** 1st story; **b** 5th story

exceeding the DCR limit depicted more potential for progressive collapse than the removal scenario at the fifth story as shown in Fig. 22.

In addition to the global DCR of the structure, this study traced the maximum member end actions (peak shear force and support bending moment) of the frames as shown in Fig. 23. From both X and Y axes, the maximum values of the member were extracted from the near sides of the removed column. In comparison, the maximum shear force was obtained from

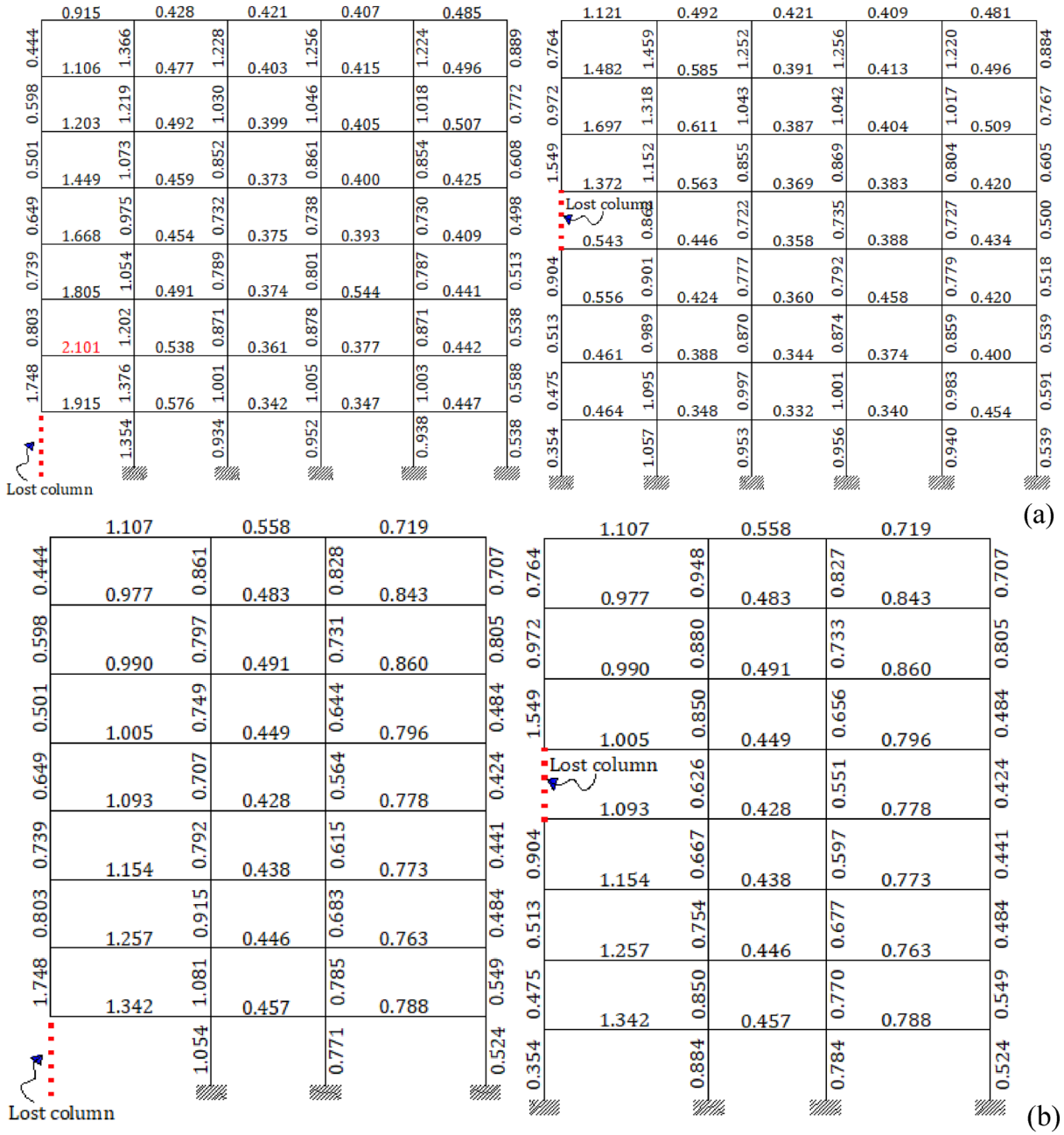

Fig. 13 DCR values for TYP_FRM column C3 removal scenario on 1st and 5th story: **a** X; **b** Y-axis

ATYP_FRM3 in which the sudden loss of first story columns C1, C2, C3, and C4 exhibited maximum shear force values of 478.38 kN, 490.09 kN, 495.13 kN, and 914.71 kN, respectively. The peak shear force value difference between ATYP_FRM3 and TYP_FRM configurations was 91%. Likewise, the maximum support bending moment from ATYP_FRM3 was 745.21 kNm, 746.44 kNm, 819.64 kNm, and 1696.17 kNm, respectively. Comparing ATYP_FRM3 with the TYP_FRM, the peak bending moment value difference is 127%.

Due to the significant impact of column removal at ground level, a detailed examination of the displacement response for this scenario is necessary. Figs. 24, 25, 26 and 27 present displacement contour plots for buildings with both typical structural configurations (SYM_FRM)

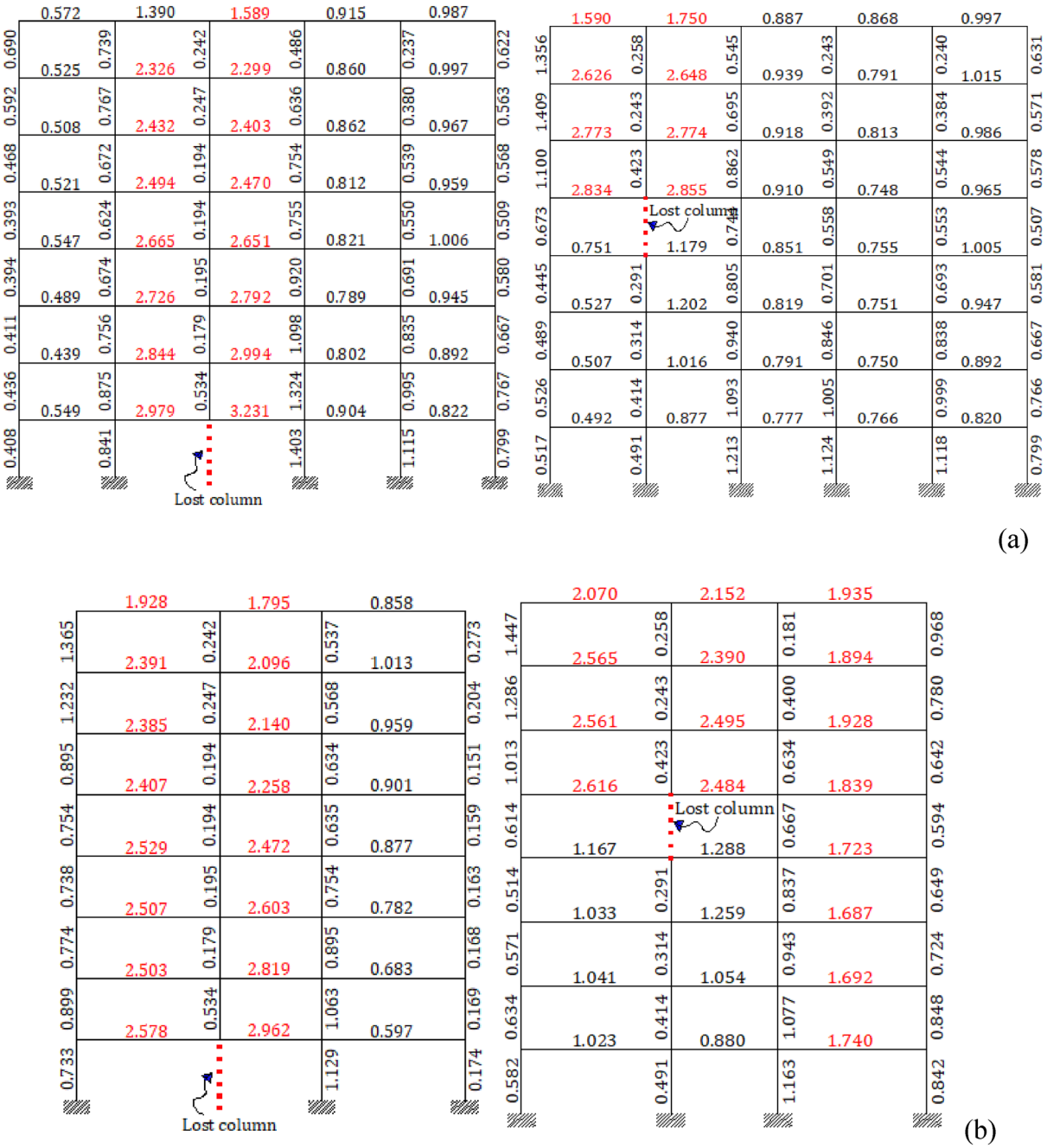

Fig. 14 DCR values for ATYP_FRM1 column C3 removal scenario on 1st and 5th story: **a** X; **b** Y-axis

and atypical structural configurations (ASYM_FRM_1, 2, and 3). Analysis of the contour plots for the loss of column C1 reveals that the maximum displacement values under the exact point of the removed column are nearly identical in magnitude. For the SYM_FRM building, the maximum displacement value is 21.80 mm, while ASYM_FRM_1 and 2 show values of 21.99 mm and 21.55 mm, respectively. In contrast, a framed building with closely spaced columns exhibit a maximum joint displacement of 8.63 mm.

In the case of column C2 loss, SYM_FRM, ASYM_FRM_1, and ASYM_FRM_3 buildings all exhibit the same maximum nodal displacement values (20 mm). Conversely, ASYM_FRM_2 reveals the least displacement value (7.05 mm) compared to the other two frame types. This reduction in nodal displacement may be

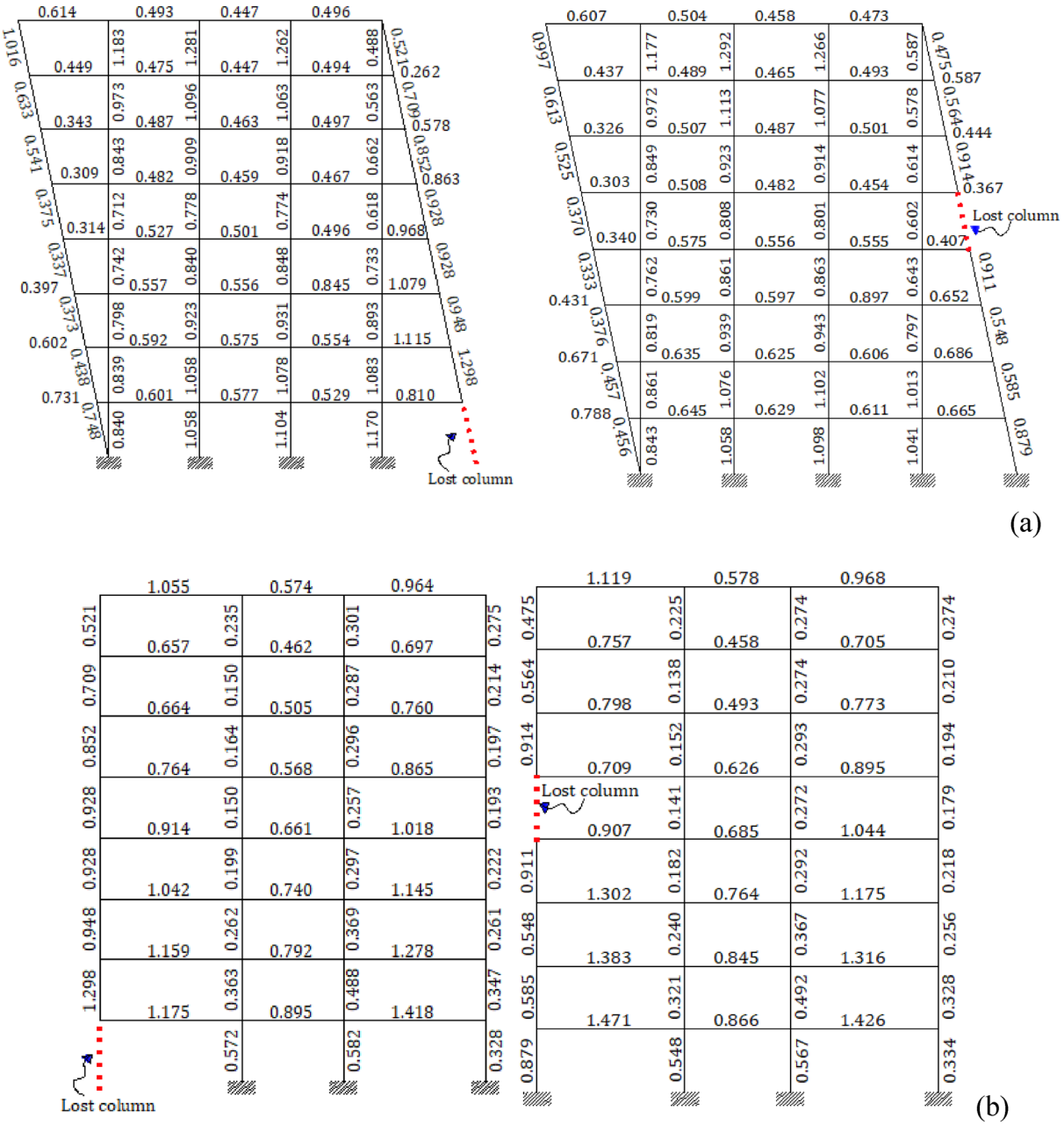

Fig. 15 DCR values for ATYP_FRM2 column C3 removal scenario on 1st and 5th story: **a** X; **b** Y-axis

attributed to the 12° inclined framing system, which, in part of the column removal location, withstands the loss of column C2 by tying the remaining structural frame elements in an intact mode.

Similarly, for the loss of column C3, SYM_FRM and ASYM_FRM_1 display maximum nodal displacements of − 21.86 mm and − 24.27 mm, respectively. In contrast, the last two atypical structural configurations (ASYM_FRM_2 and ASYM_FRM_3) demonstrate infinitesimal joint displacement values. These minimal displacements are a result of the atypical structural layouts, which enable the frame system to be tightly connected and stiffer against deformation beneath the exact point of the removed column.

Furthermore, in the case of column C4 loss, SYM_FRM, ASYM_FRM_1, and ASYM_FRM_2 structural

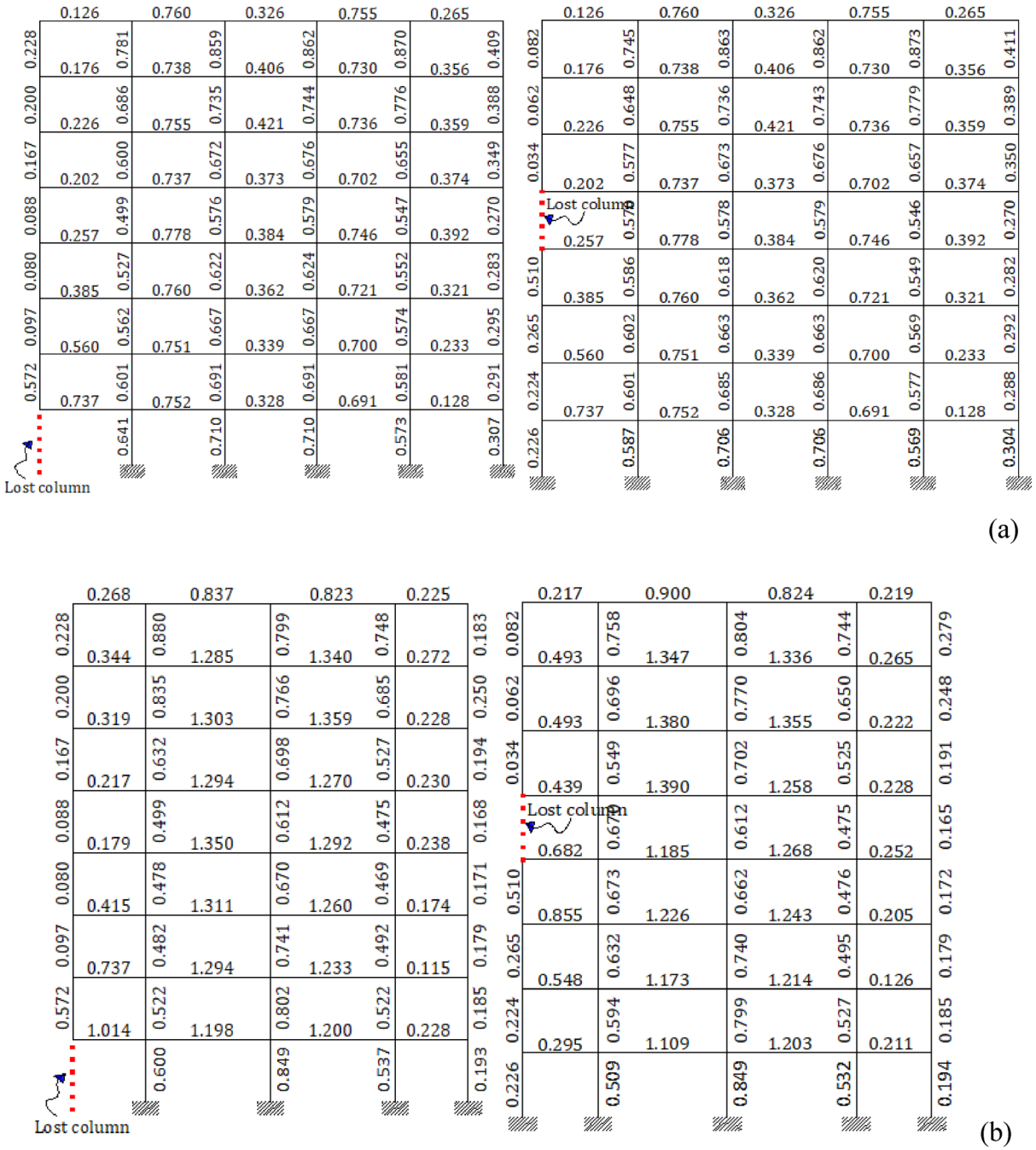

Fig. 16 DCR values for ATYP_FRM3 column C3 removal scenario on 1st and 5th story: **a** X; **b** Y-axis

configurations exhibit a maximum displacement value under the exact point of the removed column of 30 mm. Conversely, the framed building system with atypical structural arrangements (ASYM_FRM_3) demonstrates a − 73.23 mm maximum nodal displacement value.

4 Conclusion

This study evaluated the progressive collapse potential of eight-story reinforced concrete framed buildings. By employing a dynamic increase factor, a linear-static approach based on the GSA guideline is utilized to investigate four instantaneous column removal scenarios at the first and fifth stories. Additionally, three new and

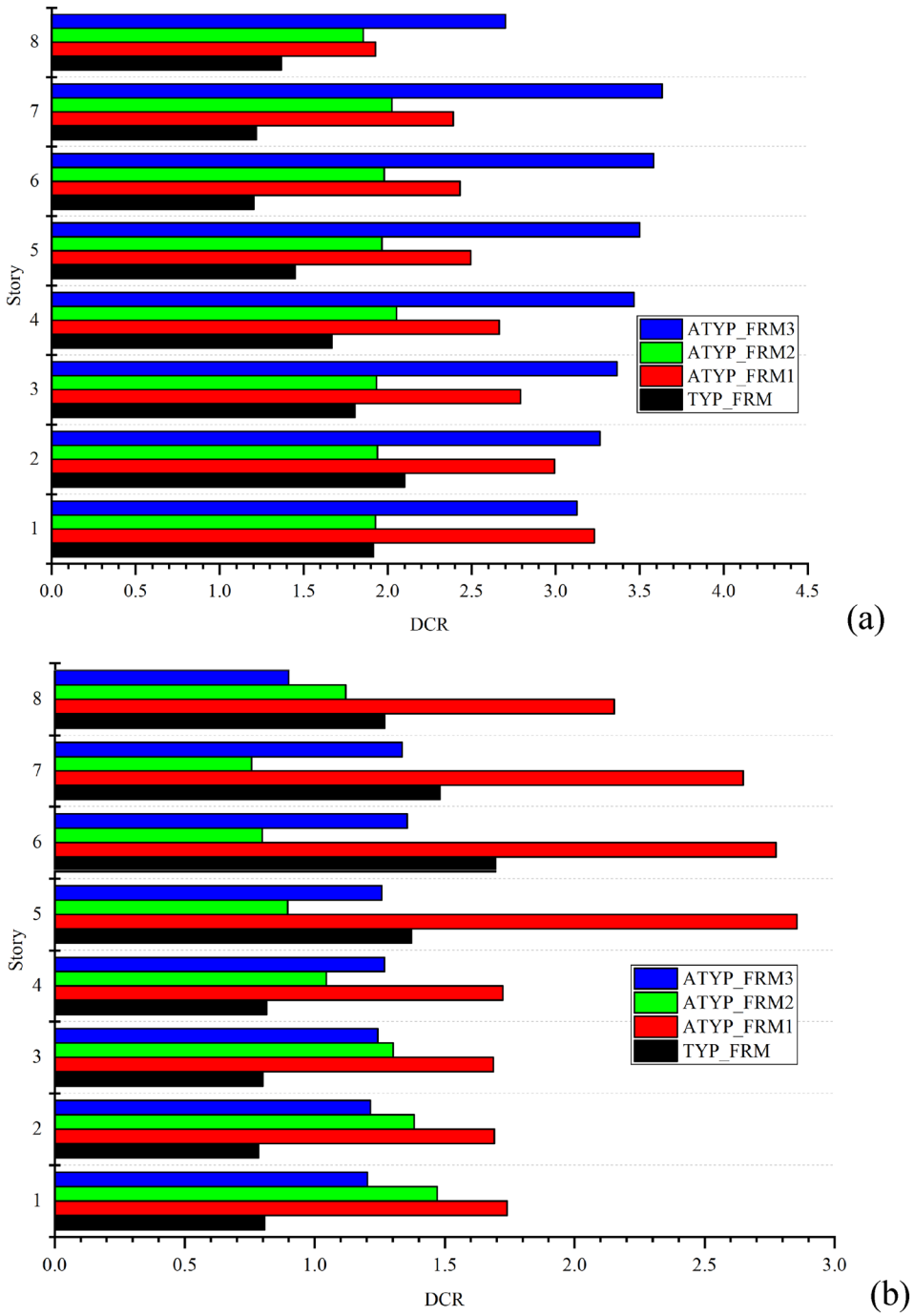

Fig. 17 Comparison of Story vs DCR for column C3 removal scenario case: **a** 1st story; **b** 5th story

unexplored atypical structural configurations are evaluated following the GSA guideline. To assess the progressive collapse potential of primary building elements, the DCR acceptance criteria limits are traced and extracted from 3D Finite Element models. The main conclusions of this study are as follows:

- Longitudinal frames with short-span beams exhibited larger DCR values compared to transverse frames with longer beam spans. The variation in DCR can be ascribed to heightened stiffness in short-span beams, leading to attract greater combined P-M2-M3

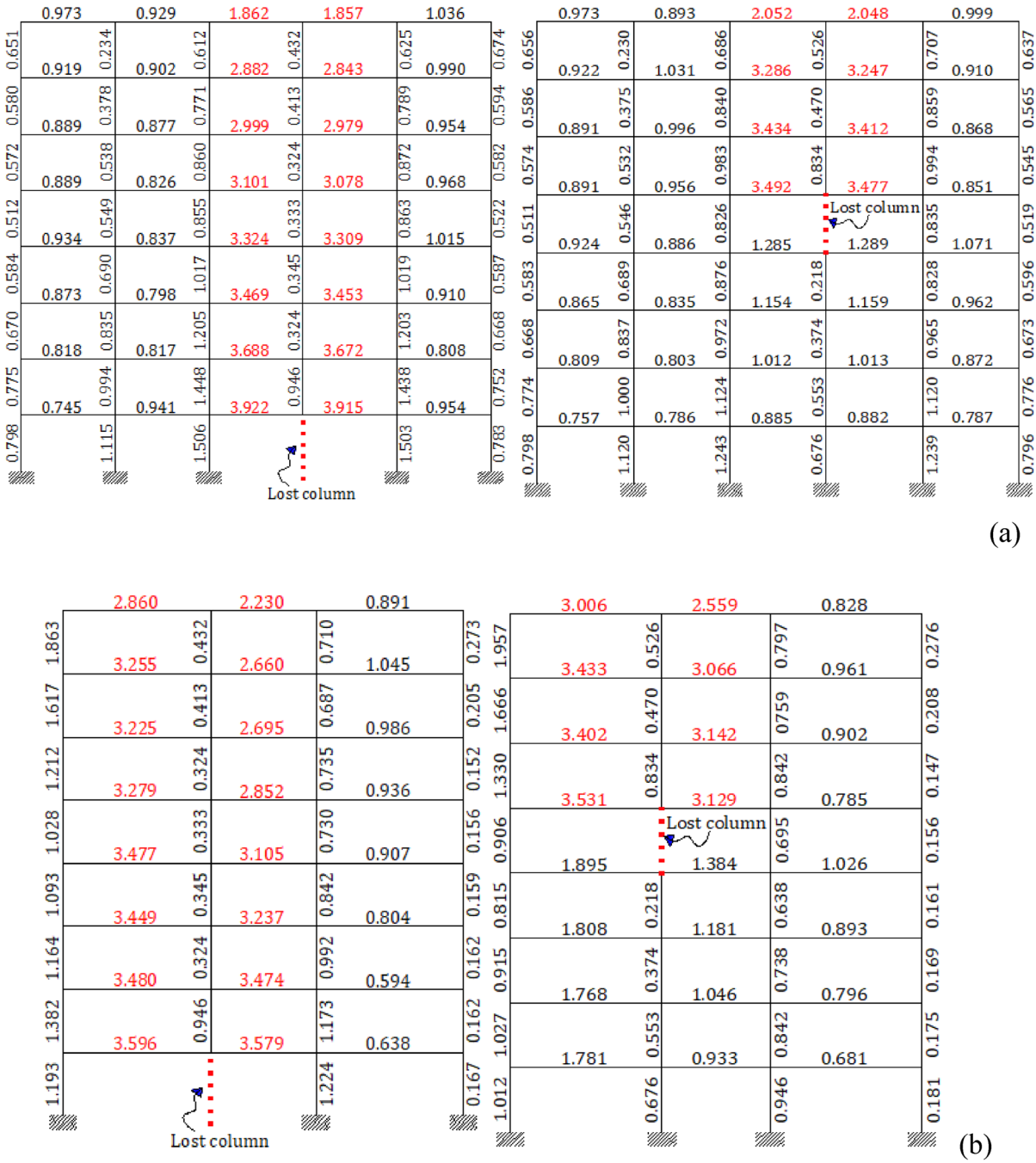

Fig. 18 DCR values for TYP_FRM column C4 removal scenario on 1st and 5th story: **a** X; **b** Y-axis

actions and consequently higher DCR values at the beam endpoints.

- For column removal at the first story, the ATYP_FRM3 structural configuration exhibited the highest DCR, with values of 2.66, 3.79, 3.6, and 8.87 for the longer side of the exterior column (C1), shorter side of the exterior column (C2), corner (re-entrant) point (C3), and interior mid-point (C4) column removal locations, respectively.
- Similarly, for column removal at the fifth story, the ATYP_FRM3 structural configuration demonstrated the highest DCR, with values of 3.57, 3.79, 3.63, and 8.88 for the longer side of the exterior column (C1), shorter side of the exterior column (C2), corner (re-entrant) point (C3), and interior mid-point (C4) column removal locations, respectively.
- Among the four sudden column removal locations, a scenario with interior column loss (C4) resulted

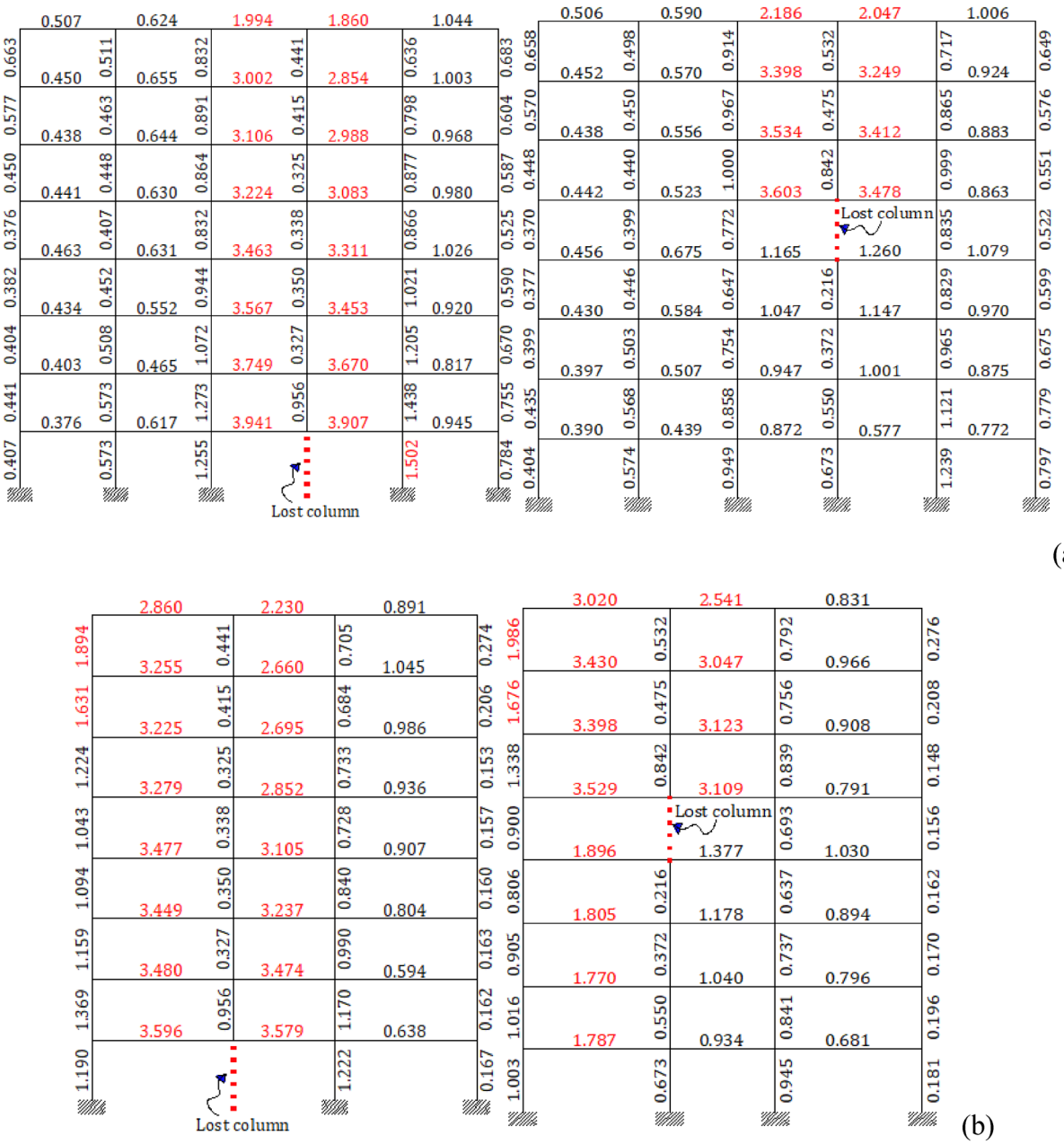

Fig. 19 DCR values for ATYP_FRM1 column C4 removal scenario on 1st and 5th story: **a** X; **b** Y-axis

in larger DCR values because of the larger tributary area of loading, and that scenario was rendered as the critical scenario for the progressive collapse of both typical and atypical frame configurations.

- Among the four column loss cases and four structural configurations, the ATYP_FRM3 structural configuration exhibited a shear failure mode. Moreover, for a structural configuration with closely spaced columns, sudden column loss at the first and fifth stories revealed a maximum member shear force of 593.4 kN and 532 kN, respectively.

Finally, it is worth noting that the current study is confined to both typical and atypical framed structures designed and detailed solely for gravitational loads. Therefore, for future research, it is advisable to expand the present study by incorporating seismic detailing provisions.

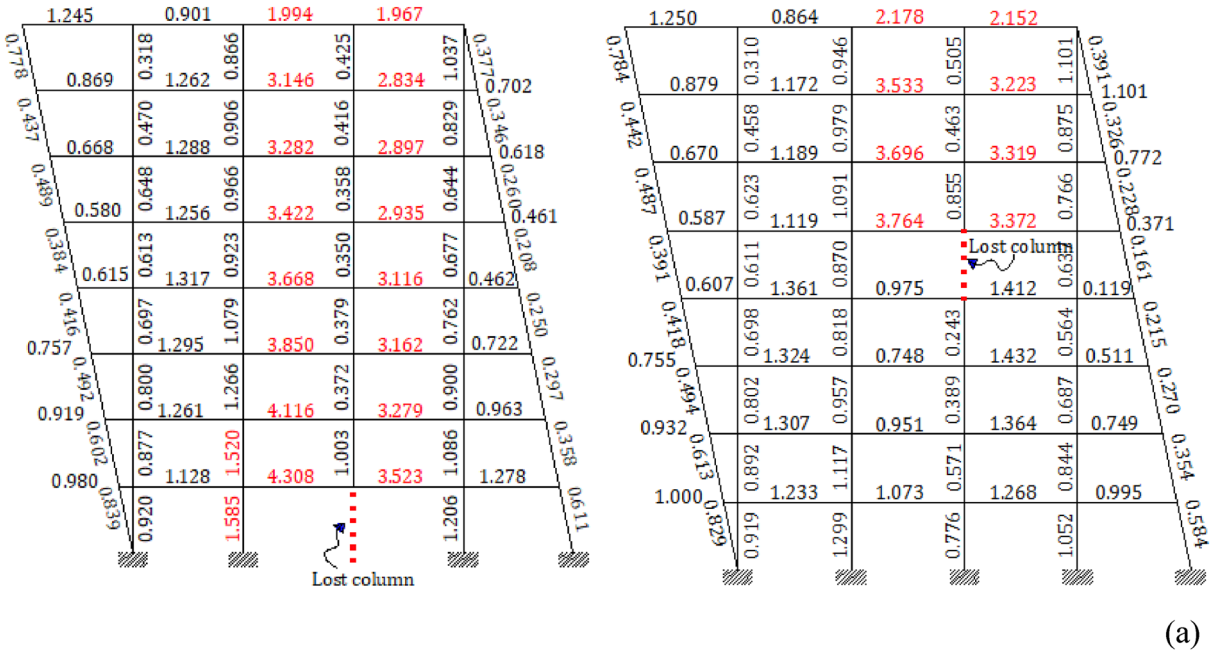

Fig. 20 DCR values for ATYP_FRM2 column C4 removal scenario on 1st and 5th story: **a** X; **b** Y-axis

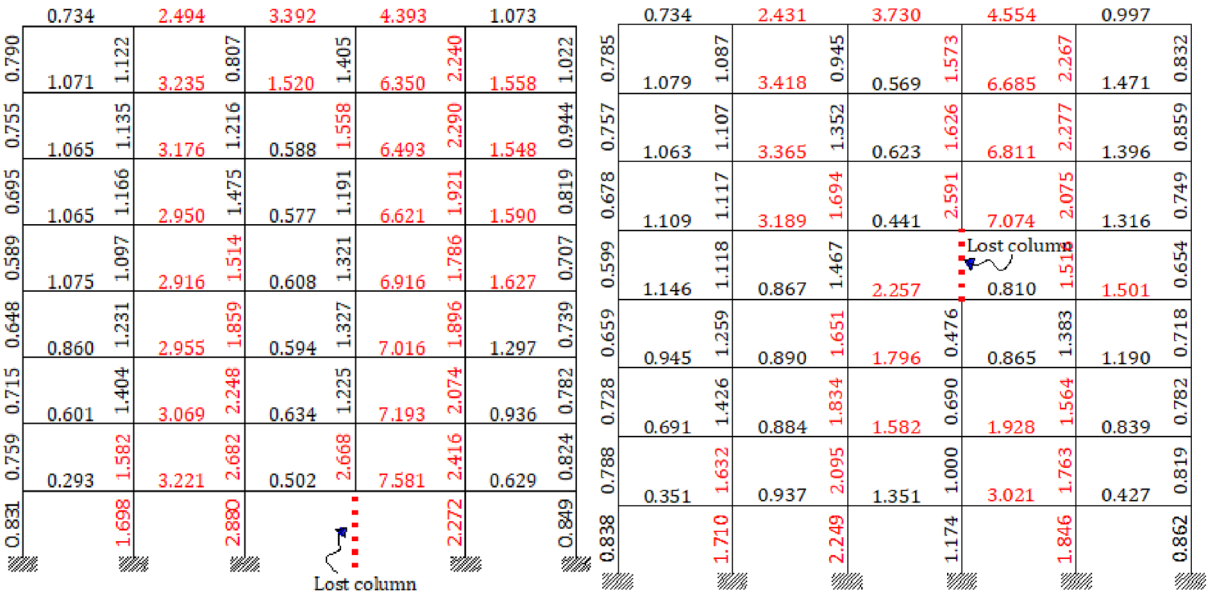

(a)

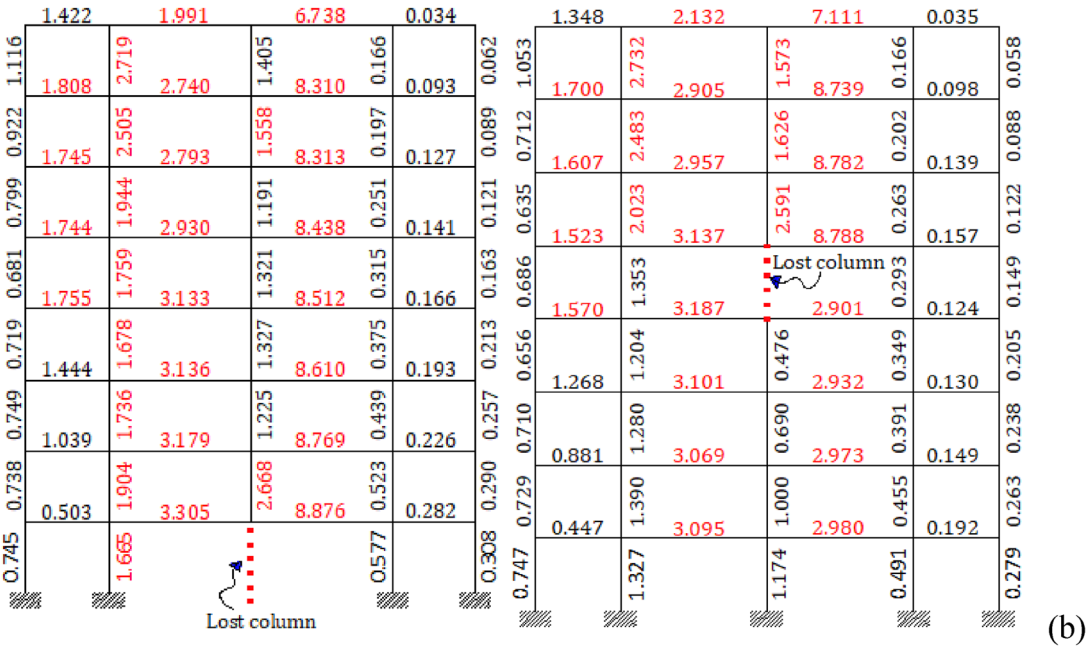

(b)

Fig. 21 DCR values for ATYP_FRM3 column C4 removal scenario on 1st and 5th story: **a** X; **b** Y-axis

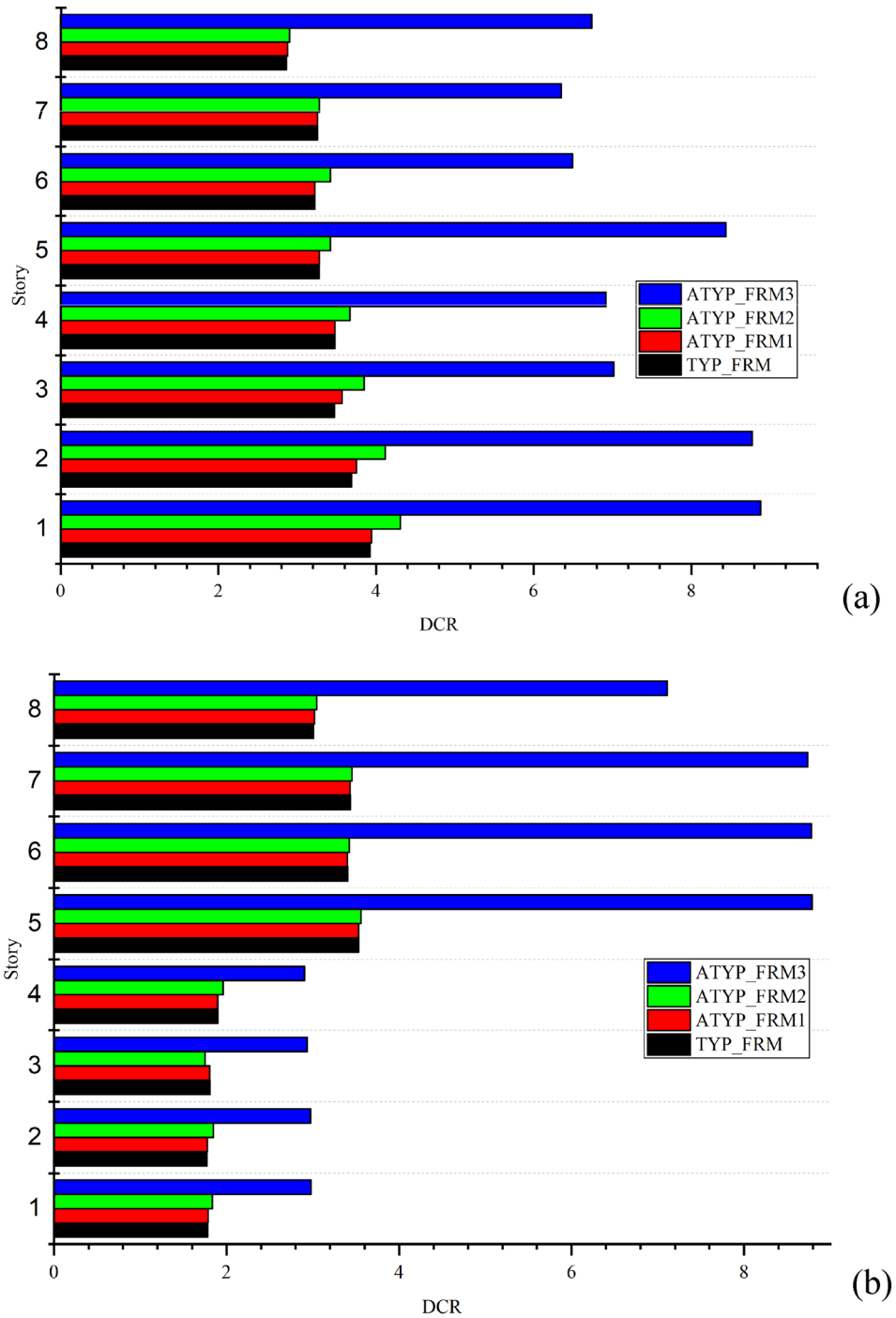

Fig. 22 Comparison of Story vs DCR for column C4 removal scenario case: **a** 1st story; **b** 5th story

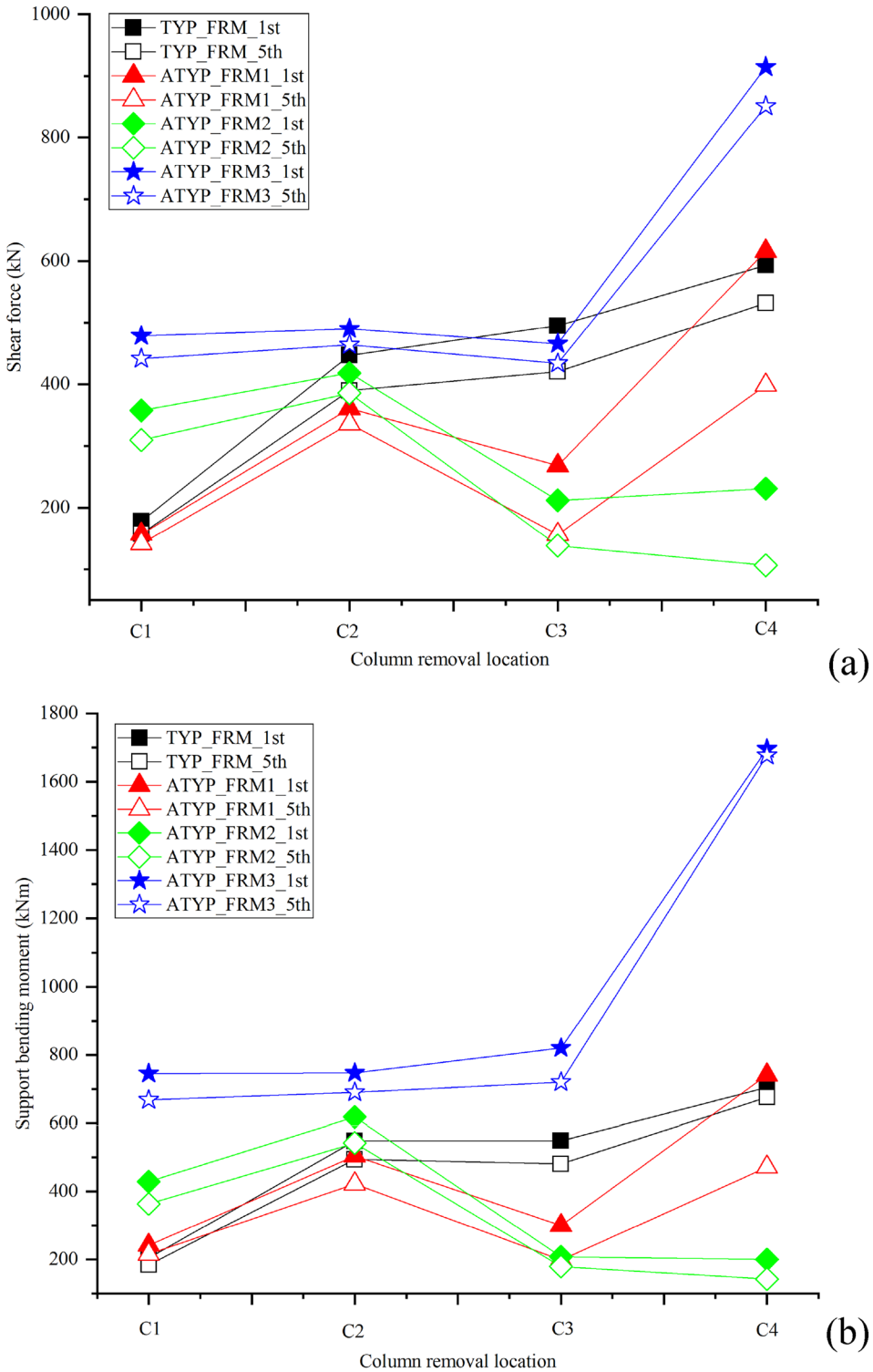

Fig. 23 Individual frame member responses for different column removal scenarios: **a** Shear force; **b** Support bending moment

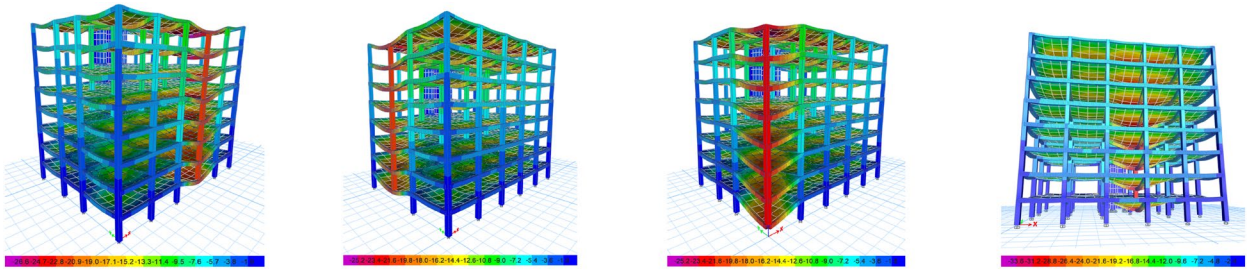

(a) (b) (c) (d)

Fig. 24 Displacement contour plots for SYM_FRM with column: **a** C1; **b** C2; **c** C3; and **d** C4 removal case

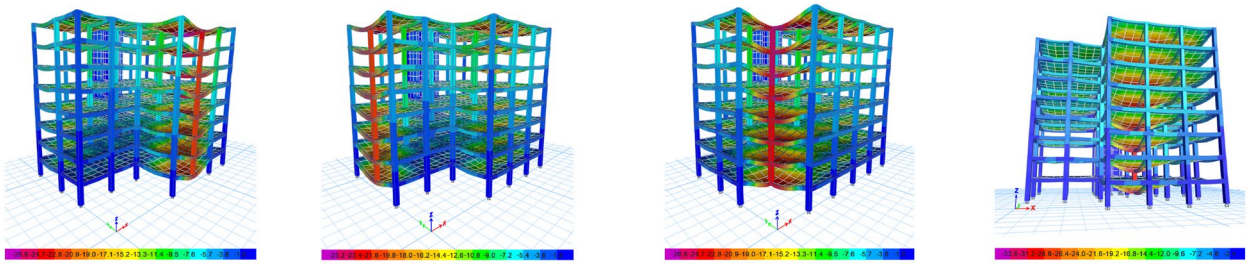

(a) (b) (c) (d)

Fig. 25 Displacement contour plots for ASYM_FRM_1 with column: **a** C1; **b** C2; **c** C3; and **d** C4 removal case

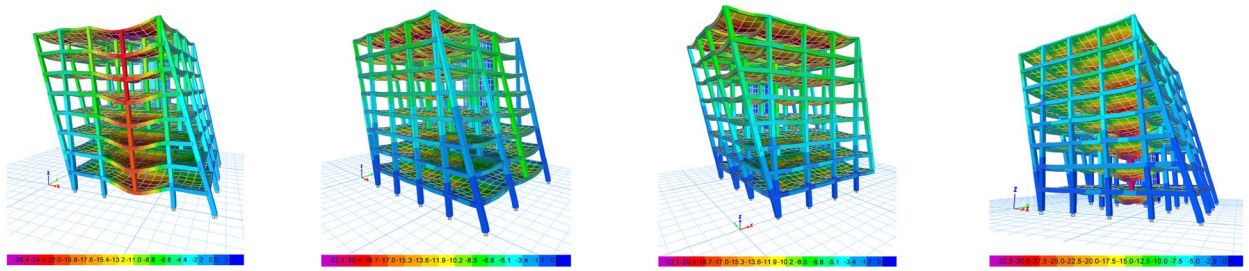

(a) (b) (c) (d)

Fig. 26 Displacement contour plots for ASYM_FRM_2 with column: **a** C1; **b** C2; **c** C3; and **d** C4 removal case

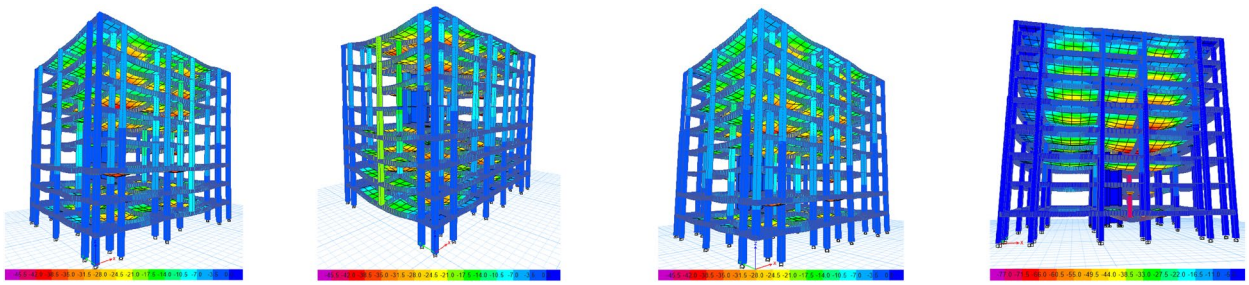

(a) (b) (c) (d)

Fig. 27 Displacement contour plots for ASYM_FRM_3 with column: **a** C1; **b** C2; **c** C3; and **d** C4 removal case

Acknowledgements
Not applicable.

Author contributions
SAD: original draft, writing, software, analysis. TAM: supervision, writing, review. GU: supervision, writing, review.

Funding
All authors declared no funding involved.

Availability of data and materials
The datasets generated during and/or analyzed during the current study are available from the corresponding author on reasonable request.

Declarations

Ethics approval and consent to participate
This article does not contain any studies with human participants or animals performed by any of the authors.

Consent for publication
We understand that the text and any pictures or videos published in the article will be used only in educational publications intended for professionals and since it's on an open-access basis, we understand that it will be freely available on the internet and may be seen by the general public.

Competing interests
The authors declare that they don't have a competing interests.

Author details
[1]Department of Civil Engineering, Debre Markos University, Debre Markos, Ethiopia. [2]Department of Civil Engineering, Addis Ababa Science and Technology University, Addis Ababa, Ethiopia. [3]Department Civil, Environmental, and Infrastructure Engineering, George Mason University, Fairfax, USA. [4]Construction Quality and Technology Center of Excellence, Addis Ababa Science and Technology University, Addis Ababa, Ethiopia.

Received: 7 September 2023 Accepted: 28 January 2024
Published online: 20 April 2024

References

ASCE. (2007). *Seismic rehabilitation of existing buildings: ASCE/SEI 41–06*. American Society of Civil Engineers.
Caredda, G., Makoond, N., Buitrago, M., Sagaseta, J., Chryssanthopoulos, M., & Adam, J. M. (2023). Learning from the progressive collapse of buildings. Developments in the Built Environment. 1–20
Djauhari, Z., Yolanda, A., Ridwan, & Yuniarto, E. (2019). "Progressive collapse of regular and irregular reinforced concrete moment frame," MATEC Web of Conferences. 276:01035
DOC. (2007). "Best practices for reducing the potential for progressive collapse in buildings," USA: National Institute of Standards and Technology-Technology Administration-U.S. Department of Commerce
DOD. (2009). *Design of buildings to resist progressive collapse: UFC 4-023-03*. Department of Defense.
EN. (2002). "Eurocode 2: Design of concrete structures—Part 1: General rules and rules for buildings pr EN1992-1-1." Brussels
Esfandiari, M., Haghighi, H., & Urgessa, G. (2023). Machine learning-based optimum reinforced concrete design for progressive collapse. *Journal of Structural Engineering*. https://doi.org/10.56748/ejse.233642
Esfandiari, M. J., & Urgessa, G. (2020). Progressive collapse design of reinforced concrete frames using structural optimization and machine learning. *Structures, 28*, 1252–1264.
Esfandiari, M. J., Urgessa, G., Sheikholarefin, S., & Manshadi, S. H. (2018). Optimization of reinforced concrete frames subjected to historical time-history loadings using DMPSO algorithm. *Structural and Multidisciplinary Optimization, 58*(5), 2119–2134.
Fu, F. (2016). *Structural analysis and design to prevent disproportionate collapse*. Taylor & Francis Group.
Gagan, B. M., & Nayak, S. G. (2019). Progressive collapse analysis of atypical reinforced concrete framed structure. *International Journal of Engineering Research & Technology (IJERT), 8*, 532–535.
Garg, S., Agrawal, V., & Nagar, R. (2020). Improved progressive collapse resistance of irregular reinforced concrete flat slab buildings under different corner column failures. *IOP Conference Series: Materials Science and Engineering*. https://doi.org/10.1088/1757-899X/1045/1/012022
Garg, S., Agrawal, V., & Nagar, R. (2020). Progressive collapse behavior of reinforced concrete flat slab buildings subject to column failures in different storeys. *Materials Today: Proceedings*. https://doi.org/10.1016/j.matpr.2020.07.692
Garg, S., Agrawal, V., & Nagar, R. (2021). Case study on strengthening methods for progressive collapse resistance of RC flat slab buildings. *Structures*. https://doi.org/10.1016/j.istruc.2020.12.049
Garg, S., Agrawal, V., & Nagar, R. (2021). Sustainability assessment of methods to prevent progressive collapse of RC flat slabs. *28th CIRP Conference on Life Cycle Engineering*. https://doi.org/10.1016/j.procir.2020.12.003
GSA. (2003). *Progressive collapse analysis and design guidelines for new federal office buildings and major modernization projects*. U.S. General Services Administration.
Haq, M., & Agarwal, A. (2019). Comparative analysis of progressive collapse of regular and irregular RC building. *GCEC*. https://doi.org/10.1007/978-981-10-8016-6_37
Kazem, A., Kazem, H., & Monavari, B. (2012). Effect of progressive collapse in reinforced concrete and steel frame structures with irregularity in shape and height. *WCEE, 15*, 1–10.
Kevins, P., & Tushar, P. (2017). Effects of irregularity on progressive collapse of RCC building. *Imperial Journal of Interdisciplinary Research (IJR), 3*(4), 1637–1647.
Khan, A. A., & Thomas, V. S. (2021). Progressive collapse performance of step back-set back building provided with secondary columns. *International Research Journal of Engineering and Technology (IRJET), 08*(07), 809–812.
Kiakojouri, F., Biagi, V. D., Chiala, B., & Sheidaii, M. R. (2020). Progressive collapse of framed building structures: Current knowledge and future prospects. *Engineering Structures*. https://doi.org/10.1016/j.engstruct.2019.110061,pp.1-21
Marchand, K. A., & Alfawakhiri, F. (2004). *Blast and progressive collapse*. American Institute of Steel Construction Inc.
Marchand, K. A., Stevens, D. J., Crowder, B., & Campbell, T. (2006). *A review and update on department of defense progressive collapse guidance* (pp. 34–37). Structure Magazine.
Obeng-Ankamah, N., Osei, J. B., & Adom-Asamoah, M. (2018). Linear static progressive collapse analysis of ductility dependent RC buildings: Case study of an 11-story building. *Journal of Structural Technology, 3*(2), 1–13.
Singh, R. S., Jamal, Y., & Khan, M. A. (2015). Progressive collapse analysis of reinforced concrete TYPmetrical and unsymmetrical framed structures by ETABS. *International Journal of Innovative Research in Advanced Engineering (IJIRAE), 2*(12), 78–83.
Starossek, U. (2009). *Progressive collapse of structures* (1st ed.). Thomas Telford Limited.
Sujeevan, D., & Kurminaidu, P. (2017). Progressive collapse analysis of reinforced concrete framed structures. *International Journal of Advance Research in Science and Engineering, 06*(08), 1988–1997.

Publisher's Note

Solomon Abebe Derseh PhD student at the Department of Civil Engineering, Debre Markos University, Debre Markos.

Tesfaye Alemu Mohammed (PhD): Associate professor at the Department of Civil Engineering, Addis Ababa Science and Technology University, Addis Ababa, Ethiopia.

Girum Urgessa (PhD): Associate professor at the Department Civil, Environmental, and Infrastructure Engineering, George Mason University, Fairfax, USA.